

**OH and Cl radicals initiated oxidation of Amyl Acetate under atmospheric conditions: Kinetics, products and mechanisms**

Journal:	<i>Environmental Science: Atmospheres</i>
Manuscript ID	EA-ART-06-2023-000082.R2
Article Type:	Paper
Date Submitted by the Author:	n/a
Complete List of Authors:	Straccia C, Vianni; Facultad de Ciencias Químicas-Universidad Nacional de Cordoba, Physical Chemistry Blanco, María; Universidad Nacional de Córdoba, Laboratorio Universitario de Química y Contaminación del Aire (L.U.Q.C.A). Instituto de Investigaciones en Físicoquímica de Córdoba (I.N.F.I.Q.C.), CONICET, Dpto. de Físicoquímica, Facultad de Ciencias Químicas; Teruel, Mariano; Facultad de Ciencias Químicas-Universidad Nacional de Cordoba, Physical Chemistry

# Environmental Science Atmospheres

## Guidelines for Reviewers



Thank you very much for agreeing to review this manuscript for *Environmental Science: Atmospheres*.

*Environmental Science: Atmospheres* is a gold open access journal publishing high quality research in fundamental and applied atmospheric science. The journal welcomes submissions that substantially advance our understanding of Earth's atmosphere, as well as research in fields such as biosphere-atmosphere chemical interactions and indoor air. More details can be found at [rsc.li/esatmospheres](https://rsc.li/esatmospheres).

The following manuscript has been submitted for consideration as a  
**FULL PAPER**

**Please note:** to support increased transparency, *Environmental Science: Atmospheres* offers authors the option of transparent peer review. If authors choose this option, the reviewers' comments, authors' response and editor's decision letter for all versions of the manuscript are published alongside the article. Reviewers remain anonymous unless they choose to sign their report.

Full papers must represent a significant development in the particular field, and should be judged according to originality, quality of scientific content and contribution to existing knowledge. Full papers do not have a page limit, but should be appropriate in length for their scientific content. Further information on article types can be found [here](#). It is essential that all articles submitted to *Environmental Science: Atmospheres* meet the significant novelty criteria; lack of novelty is sufficient reason for rejection. Please consider these high standards when making your recommendation to accept, revise, or reject.

When preparing your report, please:

- **Use the [journal scope](#)** to assess the manuscript's suitability for publication in *Environmental Science: Atmospheres*.
- **Comment on the originality, importance, impact and reliability** of the science. English language and grammatical errors do not need to be discussed, except where it impedes scientific understanding.
- **State clearly whether you think the paper should be accepted or rejected**, giving detailed comments that will both help the Editor to make a decision on the paper and the authors to improve it.
- **Inform the Editor** if there is a conflict of interest, a significant part of the work you cannot review with confidence, or if parts of the work have previously been published.
- **Provide your report rapidly** within the specified deadline, or inform the Editor if you are unable to do so.

Best regards,

**Professor Neil Donahue**  
Editor-in-Chief  
Carnegie Mellon University, USA

**Emma Eley**  
Executive Editor  
Royal Society of Chemistry, UK

Contact us

Please visit our [reviewer hub](#) for further details of our processes, policies and reviewer responsibilities as well as guidance on how to review, or click the links below.



## **Environmental Significance**

Reactivity information, SAR estimations and free energy relationships, together with a detailed understanding of products and atmospheric pathways, is necessary for a thorough assessment of the atmospheric impact of saturated esters to the air. In this study, the rate coefficients of the amyl acetate oxidation, initiated by Cl atoms and OH radicals, were determined under quasi-real atmospheric conditions using different experimental methodology. The atmospheric lifetime of the saturated ester studied determines their contribution to the average ozone production. Furthermore, small aldehydes such as formaldehyde, acetaldehyde, propionaldehyde and butyraldehyde are products reaction and secondary pollutants, could affect air quality and other environmental compartments. Aldehydes, as highly reactive compounds in the atmosphere, can contribute to the atmospheric oxidation capacity as well as to the formation of tropospheric ozone and other photooxidants of the photochemical smog.

**INFIQC**

Universidad Nacional de Córdoba  
Ciudad Universitaria- 5000 Córdoba. Argentina  
Teléfono: +54 - 351 – 5353866 – int. 53526  
Fax: +54 - 351 - 4334188  
E-mail : mariano.teruel@unc.edu.ar

Dr. Tzung-May Fu  
Associate Editor  
Environmental Science: Atmospheres  
Royal Society of Chemistry

Córdoba, 13<sup>th</sup> August 2023.

Manuscript ID: EA-ART-06-2023-000082

**OH and Cl radicals initiated oxidation of Amyl Acetate under atmospheric conditions:  
Kinetics, products and mechanisms**

Vianni G. Straccia, C.<sup>1</sup>, María B. Blanco<sup>1,2</sup> and Mariano A. Teruel<sup>1\*</sup>

Dear Dr. Tzung-May Fu,

Please find enclosed the mentioned revised manuscript considering the comments of the two Reviewers.

We have considered the comments of the reviewer 2, for which we are most grateful, as follows:

**Reviewer #2:****Minor Comments:**

1. The Authors took the suggestion of saying coefficients instead of coefficient (Environmental Significance) but the verb remains in singular (was instead of were).

**Reply:** The verb “was” was modified as suggested by “were”.

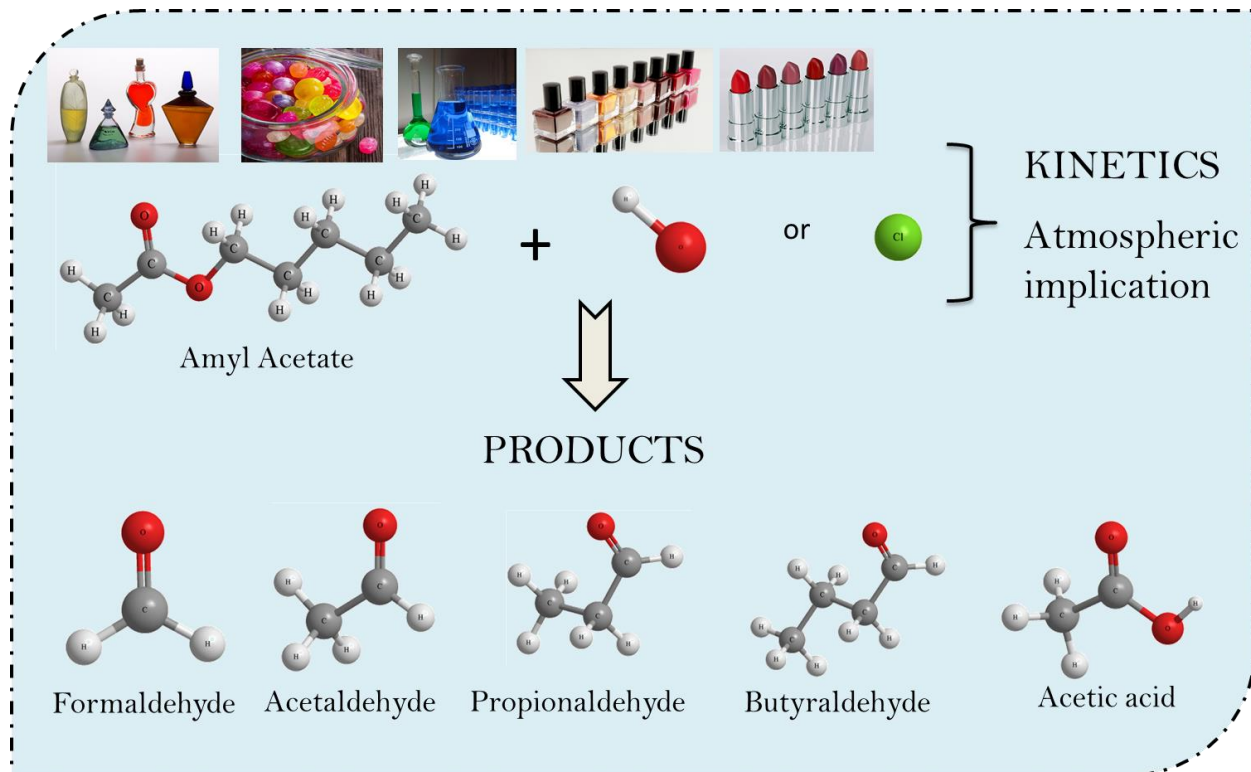
2. In Table 3 and Figure 3 it seems that the authors consider them as different substances. In fact, the revised version of the manuscript contains in Table 3 and Figure 3 two results for AA. Therefore, I consider that the relative weight of AA in the equation 13 is higher than the others acetates and ketones. This should be fixed.

**Reply:** As the reviewer commented, 2 values for AA were presented in Table 3 and in Figure 3. To avoid confusion, it was decided to remove the previously reported value for AA from Table 3 and Figure 3. Only the value determined in this work is retained.

3. I also reiterate the request to include the  $r^2$  values for the linear fits ( $\ln[AA]_0/[AA]_t$  versus  $\ln[Reference]_0/Reference]_t$ ). The authors say that they have included it in Figure 1a but it does not appear in the manuscript.

**Reply:** As the reviewer the  $r^2$  values were added in the figures 1 and 2 of the revised manuscript.

When hydrogenated esters are released into the atmosphere, they may be oxidized by OH radicals and Cl atoms, forming aldehydes and acids that have a negative local, regional, and worldwide environmental impact.



1            **OH and Cl radicals initiated oxidation of Amyl Acetate under**  
2            **atmospheric conditions: Kinetics, products and mechanisms**

3            Vianni G. Straccia, C.<sup>1</sup>, María B. Blanco<sup>1,2</sup>, and Mariano A. Teruel<sup>1\*</sup>

4            <sup>1</sup>(L.U.Q.C.A), Laboratorio Universitario de Química y Contaminación del Aire. Instituto  
5            de Investigaciones en Fisicoquímica de Córdoba (I.N.F.I.Q.C.), Dpto. de Fisicoquímica.  
6            Facultad de Ciencias Químicas, Universidad Nacional de Córdoba. Ciudad Universitaria,  
7            5000 Córdoba, Argentina.

8            <sup>2</sup> Institute for Atmospheric and Environmental Research, University of Wuppertal, DE-  
9            42097 Wuppertal, Germany.

10           **Fax: (+54) 351-4334188**

11           **\*e-mail: [mariano.teruel@unc.edu.ar](mailto:mariano.teruel@unc.edu.ar)**

12

13

14

15

16

17

18

19

20

21

22

23

24

25

26

27

28

29

30            **OH and Cl radicals initiated oxidation of Amyl Acetate under**  
31            **atmospheric conditions: Kinetics, products and mechanisms.**

32            Vianni G. Straccia, C.<sup>1</sup>, María B. Blanco<sup>1,2</sup>, and Mariano A. Teruel<sup>1\*</sup>

33            <sup>1</sup>(L.U.Q.C.A), Laboratorio Universitario de Química y Contaminación del Aire. Instituto  
34            de Investigaciones en Fisicoquímica de Córdoba (I.N.F.I.Q.C.), Dpto. de Fisicoquímica.  
35            Facultad de Ciencias Químicas, Universidad Nacional de Córdoba. Ciudad Universitaria,  
36            5000 Córdoba, Argentina.

37            <sup>2</sup> Institute for Atmospheric and Environmental Research, University of Wuppertal, DE-  
38            42097 Wuppertal, Germany.

39            **Fax: (+54) 351-4334188**

40            \*e-mail: **[mariano.teruel@unc.edu.ar](mailto:mariano.teruel@unc.edu.ar)**

41

42

43

44

45

46

47

48

49

50

51

52

53

54

55

56

57

58



**59 Abstract**

60 The relative rate coefficients of the gas-phase reaction of amyl acetate, (AA),  $\text{CH}_3\text{COO}(\text{CH}_2)_4\text{CH}_3$   
61 with OH radicals and Cl atoms were determined at  $(298 \pm 2)$  K and 1000 mbar of pressure. The  
62 experiments were developed in two different atmospheric Pyrex chambers coupled with “*in situ*”  
63 Fourier Transform Infrared (FTIR) spectroscopy and Gas Chromatography equipped with flame  
64 ionization detection (GC-FID). The rate coefficients obtained from the average of different  
65 experiments were (in units of  $\text{cm}^3 \cdot \text{molecule}^{-1} \cdot \text{s}^{-1}$ ):  $k_{AA + \text{OH-FTIR}} = (6.00 \pm 0.96) \times 10^{-12}$ ;  $k_{AA + \text{OH-GC-FID}} =$   
66  $(6.37 \pm 1.50) \times 10^{-12}$  and  $k_{AA + \text{Cl-GC-FID}} = (1.35 \pm 0.14) \times 10^{-10}$ . Additionally, product studies were  
67 completed for the Cl-initiated oxidation of AA, in similar conditions of the kinetic experiments by  
68 Gas Chromatography coupled with a mass detector (GC-MS) with Solid Phase Micro Extraction  
69 (SPME). Acetic acid, formaldehyde, acetaldehyde, propionaldehyde, and butyraldehyde were the  
70 main products identified. Complementary Structure activity relationships (SAR) were developed to  
71 compare with the experimental kinetic results and to clarify the individual reactivity sites of the ester.  
72 The atmospheric oxidation pathways of the AA are postulated and discussed taking into account the  
73 observed products and the SAR estimations. The initial pathway for the degradation of AA initiated  
74 by Cl atoms and OH radicals occurs via H-atom abstraction at  $-\text{C}(\text{O})\text{OCH}_2-$  (C1);  $-\text{CH}_2-$  (C2);  $-\text{CH}_2-$   
75 (C3); and  $-\text{CH}_2\text{CH}_3-$  (C4) moieties.

76 The atmospheric implications of the reactions studied were evaluated by the estimation of their  
77 tropospheric lifetimes toward OH radicals and Cl atoms to be:  $\tau_{\text{OH}} = 22$  and  $\tau_{\text{Cl}} = 62$  hours.  
78 Consequently, the estimated average ozone production ( $[\text{O}_3] = 2.15$ ) suggests a potential contribution  
79 of these compounds emission to the formation of photochemical smog. On the other hand, the  
80 Photochemical Ozone Creation Potential (POCP) for AA was calculated to be  $\text{POCP} = 70.2$ . A  
81 moderate risk of photochemical smog production suggests that this ester could be harmful to the  
82 health and the biota in urban environments.

83 **Keywords:** Esters reactivity, SAR, GC-FID/MS, *in situ* FTIR, Free energy relationships, POCP.

## 84 **1 Introduction**

85 The atmosphere is filled with Volatile Organic Compounds (VOCs), which are released from several  
86 anthropogenic or natural sources. Numerous VOCs can undergo photochemical reactions that result  
87 in the creation of ozone and other harmful byproducts when combined with sunlight radiation and  
88 molecular oxygen. These VOCs react with hydroxyl radicals (OH), which is the main atmospheric  
89 sink and where ozone or other products are formed. Additionally, other atmospheric oxidants,  
90 including Cl atoms, NO<sub>3</sub> radicals, and O<sub>3</sub> molecules could react with these VOCs<sup>1</sup>.

91 Acetates are a type of VOCs that are extensively utilized in various industrial procedures, primarily  
92 as solvents and in the production of fragrances and flavors. In nature, vegetation also generates these  
93 substances<sup>2</sup>. AA is used as a cosmetic product, mainly in nail polishes, enamels, and lacquer.  
94 Additionally, it serves as a solvent in nail enamel remover and employed in inks, adhesives or  
95 thinners<sup>3</sup>.

96 The atmospheric oxidation of AA, which is most likely to be initiated by OH radicals or Cl atoms,  
97 may have an impact on the production of ozone and other photochemical smog byproducts in urban  
98 areas.

99 To assess the effects of anthropogenic and biological factors on air quality, it is necessary to combine  
100 kinetic data with mechanistic information about the overall oxidation process at atmospheric pressure  
101 and room temperature.

102 In the present work, we present relative rate coefficient data for the reactions of the OH radical and  
103 Cl atoms with AA at (298 ± 52) K and 1000 mbar of pressure, using *in situ* FTIR spectroscopy and  
104 GC-FID, as analytical techniques. In addition, product studies and SAR estimations were developed  
105 for the first time for the Cl-initiated oxidation of AA to postulate the atmospheric chemical  
106 mechanism of this ester at NO<sub>x</sub> –free conditions.

107 The atmospheric lifetimes of AA were calculated using the experimental rate coefficients determined  
108 in this work to assess the potential consequences of the studied reactions on the atmosphere. The  
109 estimation of  $[O_3]$  and POCP will assess the local, regional and/or global environmental implications  
110 of the reactions studied.

## 111 **2 Experimental Section**

112 All the experiments were performed in a 405 L and 480 L Pyrex glass reactors at  $(298 \pm 2)$  K and  
113 1000 mbar = 1 atmosphere of pressure. A complete description of the reactor can be found elsewhere.<sup>4</sup>  
114 and only a brief explanation are given here. The chamber is composed of a cylindrical borosilicate  
115 glass vessel of 1.5 and 3 m. The reactors are surrounded by fluorescence lamps, which emit at a  
116 maximum of 360 nm. The radicals are produced by the radiation of the lamps. The 405 L reactor is  
117 coupled to a gas chromatograph equipped with flame ionization detection Shimadzu GC-2014B,  
118 using an Rtx-5 capillary column (fused silica G27, 30 m  $\times$  0.25 mm 0.25  $\mu$ m) using SPME as a  
119 sampling method, the gray fiber is composed of Divinylbenzene/Carboxen/Polydimethylsiloxane  
120 (DVB/CAR/PDMS).

121 On the other hand, the 480 L reactor is coupled to an *in situ* Thermo Nicolet Nexus spectrometer  
122 brand equipped with a liquid Nitrogen-Cooled Mercury-Cadmium-Telluride (MCT) detector was  
123 used to observe the loss of the reactants, and the appearance of products. This reactor has a support  
124 system for multiple reflection mirrors type "White". This system lets many reflections inside the  
125 reactor grow the optical path, which allow us to work with lower concentrations of few ppm of VOCs  
126 of interest.

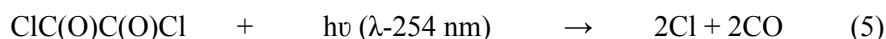
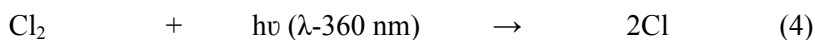
127 Using both reactors with different analytical techniques, the determination of the rate coefficients  
128 were performed by the relative method. With this method, the rate coefficient of AA could be  
129 determined indirectly from their relationship with the rate coefficient of a reference reaction.  
130 Therefore, AA and the reference compounds (ethylene, dimethyl ether, Z-1,2- dichloroethylene, and  
131 trichloroethylene) react with OH radicals or Cl atoms competitively as the following:



132 OH radicals were generated by photolysis of  $\text{H}_2\text{O}_2$  at 254 nm as follows:



133 Cl atoms were generated by UV photolysis of oxalyl chloride ( $\text{ClCOCOCl}$ ) and/or  $\text{Cl}_2$



134 Considering that reactions (1) and (2) are the only reactions that consume the reactants, it is possible  
135 to determine the relative rate coefficient of the reactions of interest as:

$$136 \quad \text{Ln} \left[ \frac{[\text{AA}]_0}{[\text{AA}]_t} \right] = \frac{k_{\text{AA}}}{k_{\text{Ref}}} \text{Ln} \left[ \frac{[\text{Ref}]_0}{[\text{Ref}]_t} \right] \quad (6)$$

137 where  $[\text{Ref}]_0$ ,  $[\text{Ref}]_t$ ,  $[\text{AA}]_0$ , and  $[\text{AA}]_t$  are the concentrations of the reference compound and AA at  
138 times  $t = 0$  and  $t$ , respectively. The slope of plots of equation 6 is the relationship between the rate  
139 coefficient of the reference compound and AA.

140 Previous tests were carried out to check that reactions (1) and (2) were the only ones that occur  
141 significantly inside the reactor. To ensure any reactions between them, the tests involved combining  
142 specified quantities of AA with various reference compounds. These mixtures were then exposed to  
143 the lamps to check the photolysis of the compound. Furthermore, no reactions between the  
144 compounds and radical's precursor in the dark were detected.

145 For product studies, mixtures of AA with oxidants in synthetic air/N<sub>2</sub> were irradiated; in a similar  
146 condition as in the kinetic study. We used GC-MS to identify the products reaction. In addition, the  
147 products were monitored with a GC-MS VARIAN Saturn 2200 with column HP-5MS, Agilent (Part  
148 19091S-433) of 30 meters in length, 0.25 mm internal diameter and film thickness 0.25 μm. The  
149 following sampling techniques were used to take gas samples from the chamber: a) the SPME was  
150 treated to derivatization using O-((perfluorobenzyl) methyl) hydroxylamine (PFBHA). For this, the  
151 microfiber was exposed for 2 minutes for headspace extraction to the derivatizing agent solution.  
152 After the SPME covered with PFBHA was exposed to the chamber with the gas reaction for 5 minutes  
153 before being injected into the GC-MS at 220 °C. b) The SPME was exposed for 10 minutes to the gas  
154 reaction by the pre-concentration method followed by the injection into the GC-MS for 2 minutes at  
155 180 °C.

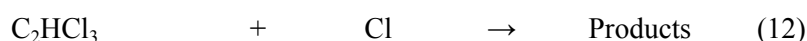
156 The initial concentrations (in ppm) used in the experiments were for AA (3) by FTIR and (6) by GC-  
157 FID, (2.4) for ethylene, (2.4) for dimethyl ether, (8) for Z-1,2- dichloroethylene, (7) for  
158 trichloroethylene, (77) for hydrogen peroxide. (1 ppm =  $2.46 \times 10^{13}$  molecule.cm<sup>-3</sup> at 298 K and 760  
159 Torr of total pressure).

160 The chemicals used in the experiments had the following purities as given by the manufacturer and  
161 were used as supplied: nitrogen (Air Liquid 99.999 %), synthetic air (Air Liquid, 99.999 %), Cl<sub>2</sub>  
162 (Messer Griesheim, 2.8), amyl acetate (Sigma-Aldrich, ≥99 %), ethylene (Sigma-Aldrich, ≥99.5%),  
163 dimethyl ether (Sigma-Aldrich, 99%), Z-1,2- dichloroethylene (Sigma-Aldrich, 97%),  
164 trichloroethylene (Supelco, 98%), and hydrogen peroxide (Interox, 85% w/w ).

## 165 **3 Results and discussion**

### 166 **3.1 Kinetics**

167 The rate coefficients for the reactions studied (1) and (2) were determined employing equation (6)  
168 with different reference compounds for each technique as follows:



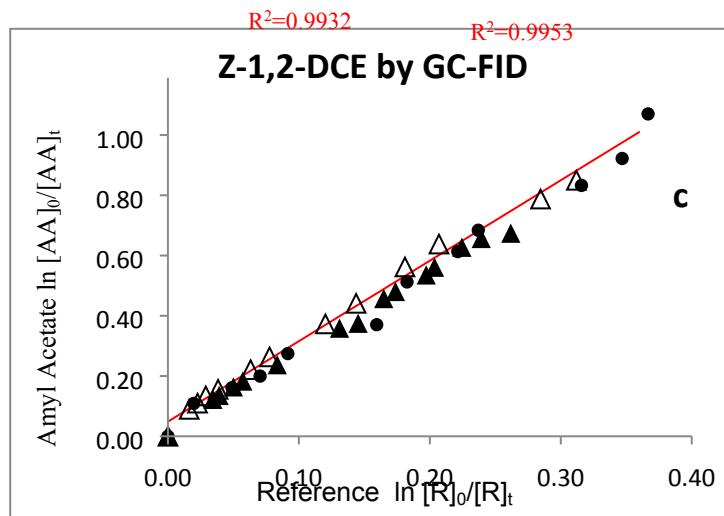
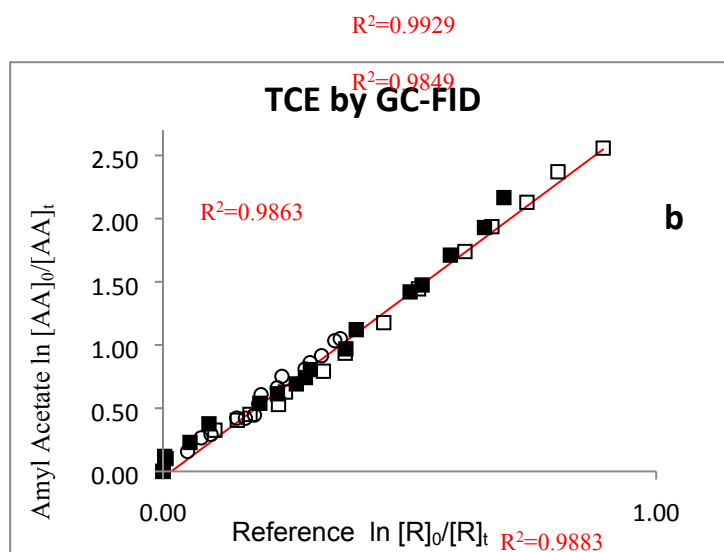
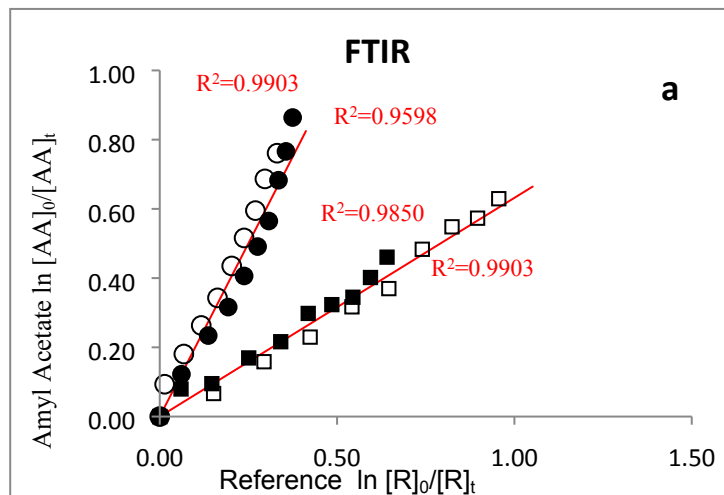
169 where  $k_7^5 = (9.00 \pm 0.30) \times 10^{-12}$ ;  $k_8^6 = (2.77 \pm 0.07) \times 10^{-12}$ ;  $k_9^7 = (2.23 \pm 0.10) \times 10^{-12}$ ;  $k_{10}^8 = (2.38 \pm$   
 170  $0.14) \times 10^{-12}$ ;  $k_{11}^9 = (9.65 \pm 0.10) \times 10^{-11}$ ;  $k_{12}^9 = (8.08 \pm 0.10) \times 10^{-11}$ . All the  $k$  values are in units of  
 171  $\text{cm}^3 \cdot \text{molecule}^{-1} \cdot \text{s}^{-1}$ .

172 The rate coefficients for the reaction under study with two oxidants were determined by the  
 173 performance of at least two experiments. Figures 1a, 1b and 1c show the plots  $\ln[\text{AA}]_0/[\text{AA}]_t$  versus  
 174  $\ln[\text{Reference}]_0/\text{Reference}]_t$  of two or three samples for each reference compound for the OH initiated  
 175 reactions. **1a** Shows the plots obtained by the FTIR technique developed using  $\text{N}_2$  with ethene and  
 176 dimethyl ether as reference compounds. **1b** and **1c** shows the plots obtained by the GC-FID technique  
 177 using synthetic air as a gas bath with trichloroethylene and Z-1,2- dichloroethylene as reference  
 178 compounds, respectively.

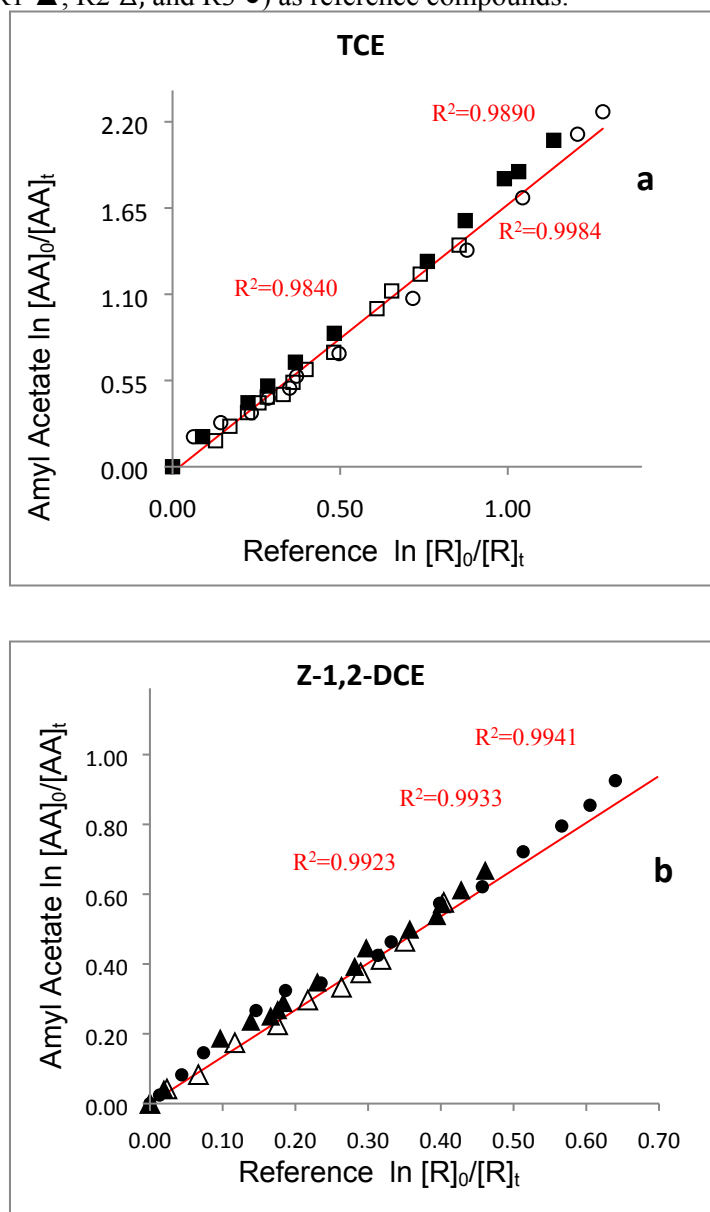
179 All plots show linearity of the straight lines obtained, with correlation coefficients close to 1 and  
 180 nearly zero intercepts indicating that secondary reactions are negligible.

181 Figure 2 shows plots obtained for the reaction of AA with Cl atoms. **2a** shows the plots of three  
 182 experiments performed using trichloroethylene as reference compounds and **2b** shows the plots  
 183 obtained using Z-1,2- dichloroethylene as reference compounds.

184



186 **Figure 1.** Kinetic data for the reaction of AA with OH radicals obtained at 298 K and atmospheric  
 187 pressure with (a) FTIR technique using ethene (R1 □ and R2 ■) and dimethyl ether (R1 ○ and R2 ●)  
 188 and (b) GC-FID technique using trichloroethylene (R1 □, R2 ■, and R3 ○) and (c) Z-1,2-  
 189 dichloroethylene (R1 ▲, R2 △, and R3 ●) as reference compounds.



190

191 **Figure 2.** Kinetic data for the reaction of AA with  $(ClC(O)C(O)Cl)$  as precursor of Cl atoms obtained  
 192 at 298 K and atmospheric pressure with GC-FID technique using (a) trichloroethylene (R1 □, R2 ■,  
 193 and R3 ○) and (b) Z-1,2- dichloroethylene (R1 ▲, R2 △, and R3 ●) as reference compounds  
 194  
 195



196 Table 1 lists the rate coefficients for the reaction of each reference compound with both oxidants. It  
 197 also includes the ( $k_{AA}/k_{reference}$ ) ratios obtained from measurements conducted using both oxidants and  
 198 techniques, along with the corresponding rate coefficient values in absolute terms. These rate  
 199 coefficient ratios are each from the average of two or three measurements. The value of the photolysis  
 200 rate for AA is also included. This value was used to correct the final value of the rate coefficient for  
 201 each reaction.

202  
 203 **Table 1.** Rate coefficient ratios  $k_{AA}/k_{reference}$ ,  $k_{photolysis}$ , rate coefficients for the reactions of OH radicals  
 204 and Cl atoms with AA using different reference compounds at  $(298 \pm 2)$  K in 760 Torr of pressure  
 205

	$k_{photolysis}$ $_{AA} \times s^{-1}$	Technique	Reference compound	$k_{reference}$ $\times 10^{12}$	$k_{AA}/$ $k_{reference}$	$k_{AA} \times 10^{12}$ $cm^3.molecul$ $e^{-1}.s^{-1}$
AA + OH	$5.29 \times 10^{-5}$	FTIR	C <sub>2</sub> H <sub>4</sub>	$9.00 \pm 0.30$	$0.66 \pm 0.04$	$5.94 \pm 0.55$
					$0.68 \pm 0.02$	$6.12 \pm 0.39$
			C <sub>2</sub> H <sub>6</sub> O	$2.77 \pm 0.07$	$2.15 \pm 0.16$	$5.96 \pm 0.59$
					$2.16 \pm 0.07$	$5.98 \pm 0.34$
					<b>Average</b>	<b><math>6.00 \pm 0.96</math></b>
	$2.42 \times 10^{-3}$	GC-FID			$2.90 \pm 0.18$	$6.47 \pm 0.69$
			C <sub>2</sub> HCl <sub>3</sub>	$2.23 \pm 0.10$	$2.91 \pm 0.14$	$6.49 \pm 0.60$
					$2.89 \pm 0.09$	$6.44 \pm 0.49$
					$2.59 \pm 0.10$	$6.16 \pm 0.60$
			Z-C <sub>2</sub> H <sub>2</sub> Cl <sub>2</sub>	$2.38 \pm 0.14$	$2.67 \pm 0.14$	$6.36 \pm 0.70$
			$2.65 \pm 0.11$	$6.31 \pm 0.63$		
			<b>Average</b>	<b><math>6.37 \pm 1.50</math></b>		
	$k_{photolysis}$ $_{AA} \times s^{-1}$	Technique	Reference compound	$k_{reference}$ $\times 10^{11}$	$k_{AA}/$ $k_{reference}$	$k_{AA} \times 10^{10}$ $cm^3.molecul$ $e^{-1}.s^{-1}$
AA + Cl	$2.27 \times 10^{-3}$	GC-FID			$1.82 \pm 0.02$	$1.47 \pm 0.03$
					$1.63 \pm 0.06$	$1.32 \pm 0.07$
			C <sub>2</sub> HCl <sub>3</sub>	$8.08 \pm 0.10$	$1.71 \pm 0.05$	$1.38 \pm 0.06$
					$1.36 \pm 0.06$	$1.31 \pm 0.07$
			Z-C <sub>2</sub> H <sub>2</sub> Cl <sub>2</sub>	$9.65 \pm 0.10$	$1.34 \pm 0.04$	$1.28 \pm 0.05$
					$1.37 \pm 0.05$	$1.32 \pm 0.06$
			<b>Average</b>	<b><math>1.35 \pm 0.14</math></b>		

206 Table 1 shows that there is good agreement between the results obtained using two different  
207 simulation chambers, four different reference compounds and *in situ* FTIR and GC-FID as detection  
208 methods. The following are the recommended average rate coefficients:

209 
$$k_{AA+OH-FTIR} = (6.00 \pm 0.96) \times 10^{-12} \text{ cm}^3 \cdot \text{molecule}^{-1} \cdot \text{s}^{-1}$$

210 
$$k_{AA+OH-GC-FID} = (6.37 \pm 1.50) \times 10^{-12} \text{ cm}^3 \cdot \text{molecule}^{-1} \cdot \text{s}^{-1}$$

211 
$$k_{AA+Cl-GC-FID} = (1.35 \pm 0.14) \times 10^{-10} \text{ cm}^3 \cdot \text{molecule}^{-1} \cdot \text{s}^{-1}$$

212 The errors shown are twice the standard deviation that results from the least-squares fit of the straight  
213 lines. The corresponding error has also been considered in the reference rate coefficients of the  
214 reaction.

215 The values of the rate coefficients of reactions with OH radicals are found to be fairly similar between  
216 2 different detection techniques, *in situ* infrared spectroscopy and gas chromatography with sample  
217 extraction by SPME.

218 For comparison purposes, the rate coefficient for the reaction of AA with OH radicals was estimated  
219 from the Structure-Activity Relationships (SAR). The rate coefficient calculation software (US  
220 Environmental Protection Agency), AOPWIN v.4.11 was used, based on the method developed by  
221 Kwok and Atkinson (1995)<sup>10</sup>. The rate coefficient calculated for H-abstraction was  $6.02 \times 10^{-12}$   
222  $\text{cm}^3 \cdot \text{molecule}^{-1} \cdot \text{s}^{-1}$ . It is shown a good concordance between the estimated rate coefficients values by  
223 SAR calculations and the obtained experimentally by FTIR  $(6.00 \pm 0.96) \times 10^{-12} \text{ cm}^3 \cdot \text{molecule}^{-1} \cdot \text{s}^{-1}$  and  
224 by GC-FID  $(6.37 \pm 1.50) \times 10^{-12} \text{ cm}^3 \cdot \text{molecule}^{-1} \cdot \text{s}^{-1}$ .

225 Furthermore, there are previous kinetic data reported for the reactions of OH radicals with AA,  
 226 performed with pulsed Laser Photolysis Laser Induced Fluorescence technique (PLP-LIF), where it  
 227 can be possible to compare with our relative determination in atmospheric conditions. The authors  
 228 reported the absolute value<sup>2</sup> of  $(7.34 \pm 0.91) \times 10^{-12} \text{ cm}^3 \cdot \text{molecule}^{-1} \cdot \text{s}^{-1}$ . On the other hand, Williams et  
 229 al. 1993, reported relative values for the rate coefficient of AA with OH radicals using Gas  
 230 Chromatography with Flame Ionization Detection<sup>11</sup> of:  $(7.53 \pm 0.48) \times 10^{-12} \text{ cm}^3 \cdot \text{molecule}^{-1} \cdot \text{s}^{-1}$ .  
 231 Additionally, previous kinetic study of AA with OH radicals reaction are reported in a doctoral  
 232 theses<sup>12</sup> by Zogka, 2016. In that theses, values of  $k_{\text{AA}+\text{OH}+1,3\text{-dioxolane}} = (6.96 \pm 0.27) \times 10^{-12} \text{ cm}^3 \cdot \text{molecule}^{-1} \cdot \text{s}^{-1}$   
 233  $^1 \cdot \text{s}^{-1}$  and  $k_{\text{AA}+\text{OH}+1\text{-pentanol}} = (7.61 \pm 0.33) \times 10^{-12} \text{ cm}^3 \cdot \text{molecule}^{-1} \cdot \text{s}^{-1}$ , were determined using relative  
 234 technique and atmospheric simulation chamber of Teflon coupled to GC-FID. Although, there are  
 235 small differences within the experimental errors, the agreement between the data obtained in this  
 236 work by GC-FID and by *in situ* FTIR with the previous relative GC-FID and PLP-LIF values is  
 237 reasonable, taking into account the experimental errors of all determinations.

238 Additionally, the predicted rate coefficient for the reaction of AA with Cl atoms was also evaluated  
 239 using the SAR method. This method was first developed to study how alkanes react with Cl atoms,  
 240 but it has been modified to take additional functional groups in more complex compounds into  
 241 account<sup>13</sup>. This method consists of computing the overall rate coefficient based on the estimation of  
 242 the rate coefficient for H-abstraction atoms from the groups  $-\text{CH}_3$ ,  $-\text{CH}_2-$  and  $>\text{CH}-$  for the  
 243 interaction of Cl atoms with alkanes<sup>14</sup>.

244 The group rate coefficients just consider the identity of the substituents next to the alkyl moiety as  
 245 follow:

$$246 \quad k(\text{CH}_3\text{-X}) = k_{\text{prim}} F(X),$$

$$247 \quad k(\text{X-CH}_2\text{-Y}) = k_{\text{sec}} F(X) F(Y),$$

$$248 \quad k(\text{X-CH-Y(Z)}) = k_{\text{tert}} F(X) F(Y) F(Z)$$

249 where,  $k_{prim} = 3.32$ ,  $k_{sec} = 8.34$ ,  $k_{tert} = 6.09$  all  $k$  in unit of ( $\times 10^{-11}$   $\text{cm}^3 \cdot \text{molecule}^{-1} \cdot \text{s}^{-1}$ ).  $F(X)$   $F(Y)$   $F(Z)$   
 250 are the moieties factor of the substituent groups  $X$ ,  $Y$ , and  $Z$ , respectively<sup>15</sup>. The SAR values were  
 251 calculated using the available substituent factors reported in many studies. Table 2 presents the factor  
 252 for each moiety compiled according to the structure of the AA,  $\text{CH}_3\text{COO}(\text{CH}_2)_4\text{CH}_3$ .

253

254

255

**Table 2.** SAR group reactivity factors for the reaction with Cl atoms.

Substituent	Factor <sub>(Cl)</sub>	Reference
(-C(O)OR)	0.12	Ifang et al, 2015 <sup>13</sup>
(RC(O)O-)	0.066	Xing et al, 2009 <sup>16</sup>
(-CH <sub>3</sub> )	1	Aschmann and Atkinson <sup>15</sup>
(-CH <sub>2</sub> -)	0.79	

256 From the data presented in Table 2 the following SAR value for the reaction of AA with Cl atoms  
 257 has been estimated:  $2.05 \times 10^{-10}$   $\text{cm}^3 \cdot \text{molecule}^{-1} \cdot \text{s}^{-1}$ . It should be observed that the estimated rate  
 258 coefficients value and the experimentally measured of  $(1.35 \pm 0.14) \times 10^{-10}$   $\text{cm}^3 \cdot \text{molecule}^{-1} \cdot \text{s}^{-1}$  are close  
 259 considering the experimental error.

260 Moreover, there are previous kinetic data reported by Zogka, 2016<sup>12</sup> for the reactions of AA with Cl  
 261 atoms. Values reported were  $k_{\text{AA}+\text{Cl}+\text{n-pentane}} = (2.07 \pm 0.04) \times 10^{-10}$   $\text{cm}^3 \cdot \text{molecule}^{-1} \cdot \text{s}^{-1}$  and  $k_{\text{AA}+\text{Cl}+\text{1-butanol}} =$   
 262  $(2.13 \pm 0.03) \times 10^{-10}$   $\text{cm}^3 \cdot \text{molecule}^{-1} \cdot \text{s}^{-1}$ . The values reported by us could be slightly lower than those  
 263 reported by Zogka. However, there is another value reported by Ifang et al. 2015. The rate coefficient  
 264 informed<sup>13</sup> of  $(1.790 \pm 0.153) \times 10^{-10}$   $\text{cm}^3 \cdot \text{molecule}^{-1} \cdot \text{s}^{-1}$  is also in agreement with the value reported in  
 265 this work.

266

267 A previous reaction trend reported by Atkinson 1986<sup>17</sup> for acetates pointed out that the rate coefficient  
 268 for the reaction of acetates with OH radicals increases with the length of the carbon chain. The  
 269 following rate coefficient values have been reported in several studies:  $\text{CH}_3\text{C}(\text{O})\text{OCH}_3$ ,  $k_{(\text{methyl acetate} + \text{OH})}^{18} = 3.5 \times 10^{-13}$ ;  
 270  $\text{CH}_3\text{C}(\text{O})\text{OCH}_2\text{CH}_3$ ,  $k_{(\text{ethyl acetate} + \text{OH})}^{19} = 1.73 \times 10^{-12}$ ;  $\text{CH}_3\text{C}(\text{O})\text{OCH}_2\text{CH}_2\text{CH}_3$ ,  $k_{(\text{propyl acetate} + \text{OH})}^{20} = 1.97 \times 10^{-12}$ ;  
 271  $\text{CH}_3\text{C}(\text{O})\text{OCH}_2\text{CH}_2\text{CH}_2\text{CH}_3$ ,  $k_{(\text{butyl acetate} + \text{OH})}^{21} = 5.20 \times 10^{-12}$ ;  
 272  $\text{CH}_3\text{C}(\text{O})\text{OCH}_2\text{CH}_2\text{CH}_2\text{CH}_2\text{CH}_3$ ,  $k_{(\text{AA} + \text{OH})\text{-Average this work}} = 6.19 \times 10^{-12}$ . All the  $k$  values are in units of  
 273  $\text{cm}^3 \cdot \text{molecule}^{-1} \cdot \text{s}^{-1}$ . That is the  $k_{\text{OH}}$  increase with the number of secondary ( $\text{CH}_2$ ) and tertiary ( $\text{C-H}$ )  
 274 bonds. On the other hand, there is a similar trend for the reactions of acetates with Cl atoms. Several  
 275 research have reported the corresponding rate coefficient values for the Cl atoms as follows:  
 276  $\text{CH}_3\text{C}(\text{O})\text{OCH}_3$ ,  $k_{(\text{methyl acetate} + \text{Cl})}^{22} = 2.20 \times 10^{-12}$ ;  $\text{CH}_3\text{C}(\text{O})\text{OCH}_2\text{CH}_3$ ,  $k_{(\text{ethyl acetate} + \text{Cl})}^{13} = 1.71 \times 10^{-11}$ ;  
 277  $\text{CH}_3\text{C}(\text{O})\text{OCH}_2\text{CH}_2\text{CH}_3$ ,  $k_{(\text{propyl acetate} + \text{Cl})}^{13} = 7.70 \times 10^{-11}$ ;  $\text{CH}_3\text{C}(\text{O})\text{OCH}_2\text{CH}_2\text{CH}_2\text{CH}_3$ ,  $k_{(\text{butyl acetate} + \text{Cl})}^{13} =$   
 278  $1.20 \times 10^{-10}$ ;  $\text{CH}_3\text{C}(\text{O})\text{OCH}_2\text{CH}_2\text{CH}_2\text{CH}_2\text{CH}_3$ ,  $k_{(\text{AA} + \text{Cl})\text{-Average this work}} = 1.35 \times 10^{-10}$ . Similar to the reaction  
 279 with OH radicals, the rate coefficient for the reaction of acetates with Cl atoms increases with the  
 280 length of the carbon chain. The values obtained in this work are consistent with the trend reported.  
 281 There is the first experimental kinetic study of the reaction of AA with Cl atoms using the relative  
 282 kinetic technique in a photoreactor coupled to FTIR spectrometers<sup>13</sup>.

### 283 3.2 Free energy relationships

284 Several studies found a linear relationship between the rate coefficients of different compounds in  
 285 reaction with OH radicals and Cl atoms<sup>23,24</sup>. In this study, Table 3 shows a relationship between  $k_{\text{OH}}$   
 286 and  $k_{\text{Cl}}$  of several acetates and ketones reported previously in the literature, including the kinetic data  
 287 for AA from the present determination. The relationship between the rate coefficients for the  
 288 reactions of OH radicals and Cl atoms is presented in Figure 3 where a significant correlation is  
 289 established. The data from Figure 3 are subjected to a least-squares analysis, which produces the  
 290 following expression:

$$\log k_{\text{OH}} = 1.1294 \log k_{\text{Cl}} - 0.0123 \quad (r^2 = 0.99) \quad (13)$$

**Table 3.** Comparison between  $k_{\text{OH}}$  and  $k_{\text{Cl}}$  of a series of acetates and ketones, together with the kinetic data for AA obtained in this work, at  $(296 \pm 2)$  K.

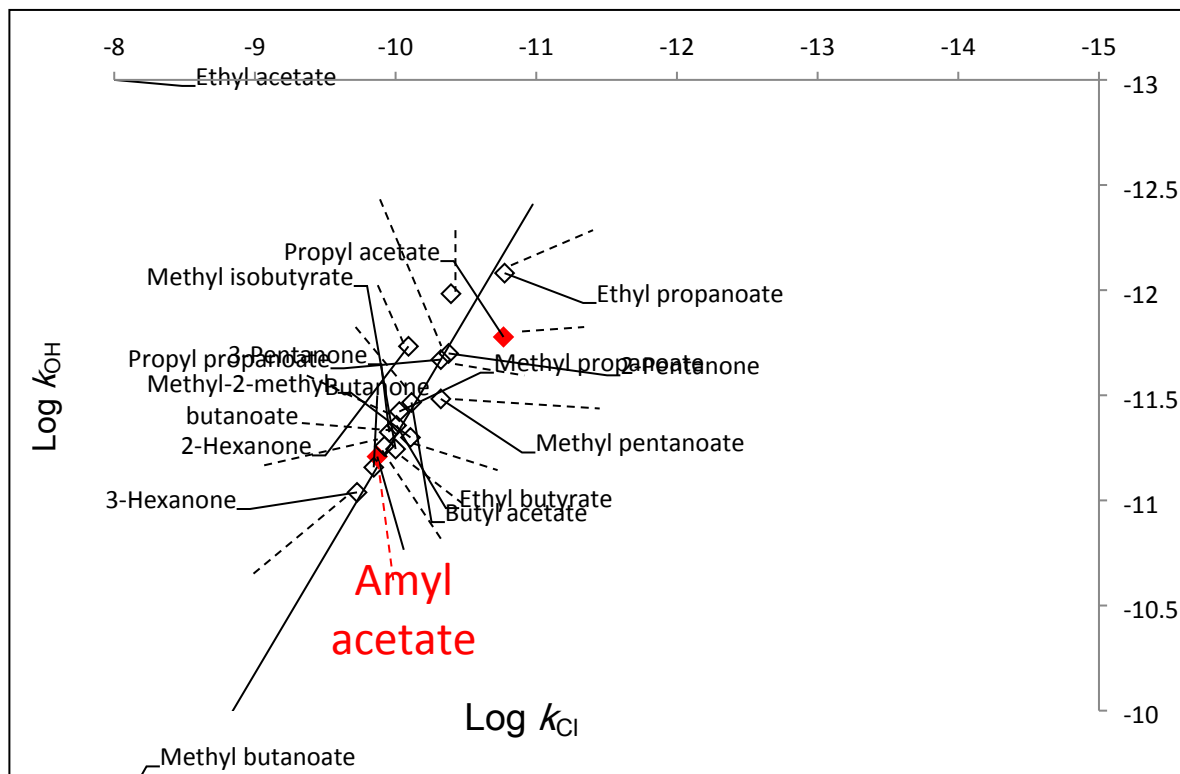
Compound	$k_{\text{Cl}}$	Ref Cl	$k_{\text{OH}}$	Ref OH
Methyl acetate	$2.20 \times 10^{-12}$	22	$3.20 \times 10^{-13}$	2
Ethyl acetate	$1.71 \times 10^{-11}$	13	$1.67 \times 10^{-12}$	2
Propyl acetate	$7.70 \times 10^{-11}$	13	$3.42 \times 10^{-12}$	2
Butyl acetate	$1.20 \times 10^{-10}$	13	$5.52 \times 10^{-12}$	2
Amyl acetate	$1.35 \times 10^{-10}$	This work	$6.19 \times 10^{-12}$	This work
Methyl butanoate	$4.77 \times 10^{-11}$	25	$3.29 \times 10^{-12}$	25
Methyl pentanoate	$7.84 \times 10^{-11}$	25	$5.02 \times 10^{-12}$	25
Methyl-2-methyl- butanoate	$9.41 \times 10^{-11}$	25	$3.78 \times 10^{-12}$	25
Methyl propanoate	$1.68 \times 10^{-11}$	13	$8.30 \times 10^{-13}$	26
Ethyl propanoate	$4.19 \times 10^{-11}$	13	$2.14 \times 10^{-12}$	27
Propyl propanoate	$9.84 \times 10^{-11}$	13	$4.40 \times 10^{-12}$	28
Ethyl butyrate	$1.00 \times 10^{-10}$	28	$5.70 \times 10^{-12}$	28
Methyl isobutyrate	$4.20 \times 10^{-11}$	28	$2.00 \times 10^{-12}$	28
2-pentanone	$1.11 \times 10^{-10}$	29	$4.74 \times 10^{-12}$	30
3-pentanone	$8.10 \times 10^{-11}$	29	$1.85 \times 10^{-12}$	30
2-hexanone	$1.88 \times 10^{-10}$	29	$9.16 \times 10^{-12}$	30
3-hexanone	$1.43 \times 10^{-10}$	29	$6.96 \times 10^{-12}$	30
Butanone	$4.04 \times 10^{-11}$	29	$1.04 \times 10^{-12}$	31

295

296 There is a direct relationship between the rate coefficients for both oxidants as it can be seen in the  
297 free energy plot for the various oxygenated compounds.

298 The good quality of the correlation between the reaction rate coefficients of OH radicals and Cl atoms  
299 is such that an estimation of the rate coefficients can be made for reactions which have not yet been  
300 investigated. In addition, this correlation shows that the degradation mechanism initiated by the Cl  
301 atoms is similar that OH radicals, *i.e.*, by the abstraction of the H atoms.

302



303

304 **Figure 3:** Free energy plots  $\log(k_{OH})$  vs.  $\log(k_{Cl})$  for the reactions with Cl and OH of acetates  
 305 and ketones reported in previous work together with the AA studied in this work (Table 3).

306

### 307 3.3. Products studies

308 Mixtures of AA with molecular chlorine in air were photolyzed to identify the oxidation products.

309 These experiments were conducted under similar conditions to the kinetic experiments.

310 Approximately 50% of consumption the original ester concentration was used in the development of

311 each study.

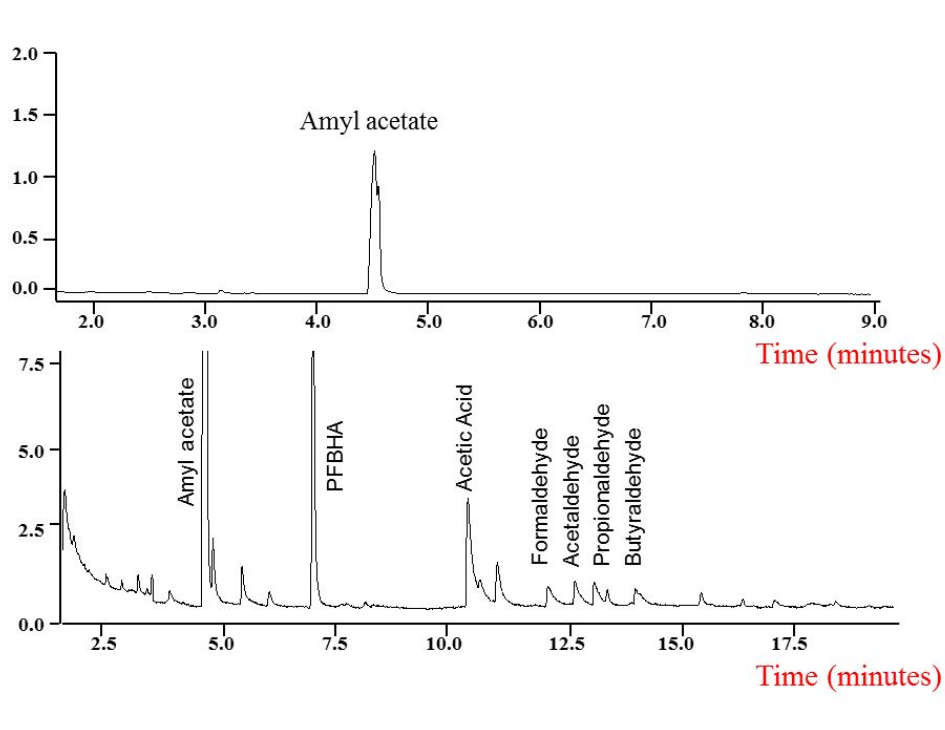
312 The atmospheric degradation of saturated esters with atmospheric oxidants is initiated by H-atoms  
313 abstraction from the alkyl groups CH; CH<sub>2</sub>; and/or CH<sub>3</sub>. This produces alkyl radicals with the  
314 following stability trend<sup>32</sup> being CH>CH<sub>2</sub>>CH<sub>3</sub>. The abstraction of H-atoms will be based on SAR  
315 estimated probability as follows; 0.7% at -CH<sub>3</sub>C(O)O-; 30% at -C(O)OCH<sub>2</sub>- (C1); 23% at -CH<sub>2</sub>-  
316 (C2); 23% at -CH<sub>2</sub>- (C3); 19% at -CH<sub>2</sub>CH<sub>3</sub>- (C4); and 3% at -CH<sub>3</sub> (C5);. These probabilities obtained  
317 from SAR estimation proposed that there will be several routes and secondary carbons will be the  
318 main pathway of H-atom abstraction.

319 GC-MS studies were developed to identify the end products of the chemical reaction between AA  
320 and Cl atoms. The SPME (DVB/CAR/PDMS) microfiber was exposed in the PFBHA before being  
321 exposed to the gas reaction in the Pyrex chamber. The products, formaldehyde, acetaldehyde,  
322 propionaldehyde, and butyraldehyde were positively identified as carbonyl oximes due to the reaction  
323 with the PFBHA (See Figures 4 and 5). The following carbonyl oximes were found: formaldehyde  
324 oxime, o-[(pentafluorobenzyl) methyl]; acetaldehyde oxime, o-[(pentafluorobenzyl) methyl];  
325 propionaldehyde oxime, o-[(pentafluorobenzyl) methyl]; and butyraldehyde oxime, o-  
326 [(perfluorobenzyl) methyl]. Acetic acid was found without derivatizing on the experiments by the  
327 pre-concentration method.



328 The mixture was photolyzed using air as bath gas and AA was detected at a retention time of 4.6 min  
329 with the matching ( $m/z$ ) ratios of 43, 55, 70, 87 and 115 (see Figures 4 and 5). The particular fragments  
330 ( $m/z$ ) of the main products at the successive retention times and the percentage of coincidence (match)  
331 are also shown in Figure 4: formaldehyde at 11.7 min, ( $m/z$ ): 47, 61, 81, 99, 117, 131, 161, 167, 181,  
332 and 225, with a match=97%; acetaldehyde at 12.9 min, ( $m/z$ ): 58, 81, 99, 117, 131, 161, 167, 181,  
333 209, and 239, with a match=90%; propionaldehyde at 13.2 min, ( $m/z$ ): 44, 54, 72, 99, 117, 131, 161,  
334 167, 181, 203, 236, and 253, with a match=95%; butyraldehyde at 14 min, ( $m/z$ ): 41, 55, 69, 86, 117,  
335 131, 161, 167, 181, 207, 222, 239, and 267, with a match=92%; and acetic acid at 10.3 min, ( $m/z$ ):  
336 29, 36, 40, 43, 45, 56, 60, and 61, with a match=92%. All of these fragments  $m/z$  are characteristic of  
337 these identified compounds<sup>33</sup>.

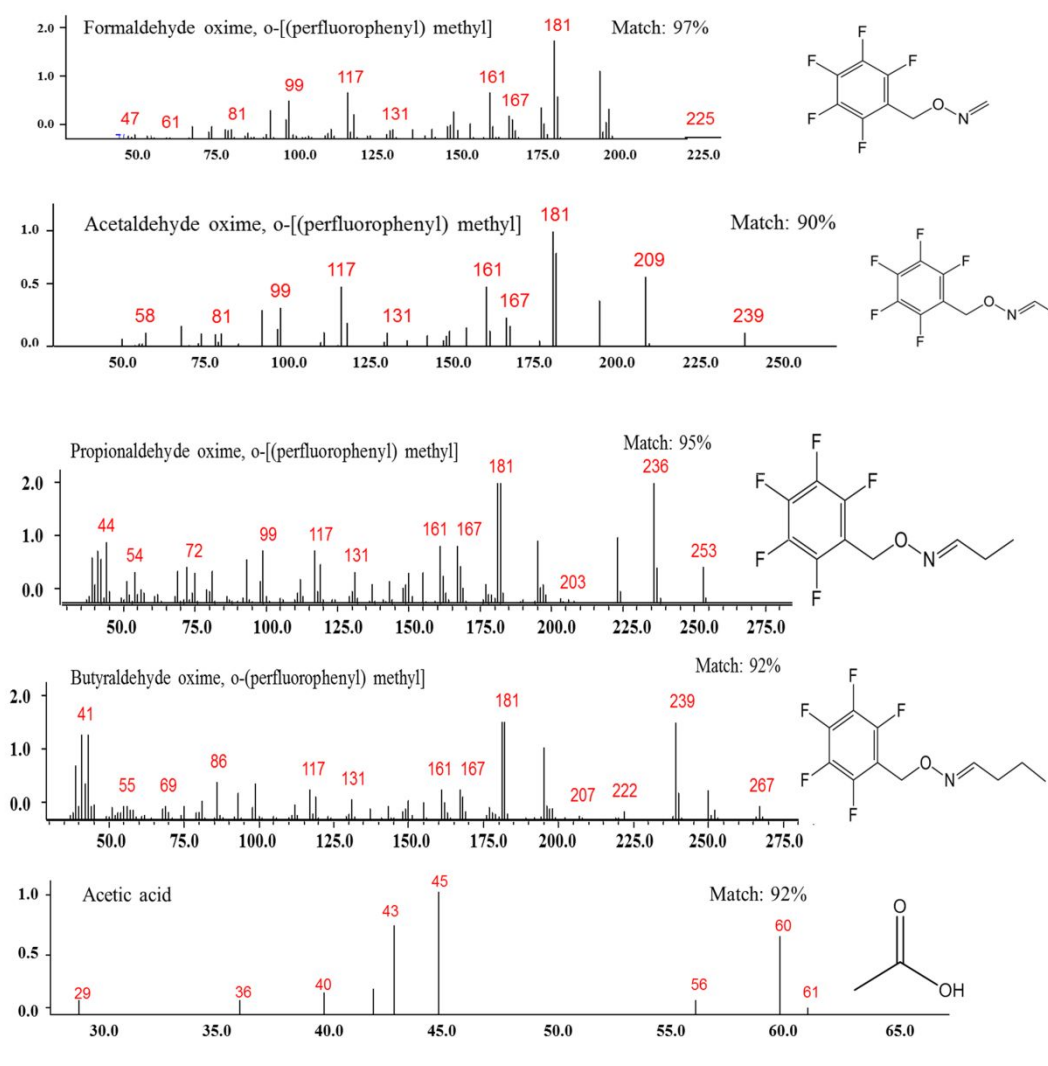
338 We postulate a degradation mechanism in Schemes 1 and 2 with four potential pathways, taking into  
339 account the products found and the SAR estimations of the reactive sites of AA.



340

341 **Figure 4.** GC-MS chromatogram of mixture of (AA + Cl<sub>2</sub>) on air, before and after photolysis.

342



343

344 **Figure 5.** Products observed and the mass spectra for formaldehyde,  
 345 propionaldehyde, butyraldehyde and acetic acid.

346 Scheme 1 shows that the reaction between Cl atoms and AA can occur via H-atom abstraction at the  
 347  $-C(O)OCH_2-$ , ( $C_1$ ), in channel A and from  $-CH_2-$  ( $C_2$ ) in channel B.

348 From channel A, the H-atoms abstraction from  $C_1$  produces the alkyl radical  
 349  $CH_3C(O)OC(\bullet)H(CH_2)_3CH_3$  followed by  $O_2$  addition to form the peroxy radicals  
 350  $CH_3C(O)OC(OO\bullet)H(CH_2)_3CH_3$  with further alkoxy radicals formation  
 351  $(CH_3C(O)OC(O\bullet)H(CH_2)_3CH_3)$ . These  $CH_3C(O)OC(O\bullet)H(CH_2)_3CH_3$  radicals can follow two  
 352 different reaction pathways: 1) decomposition, with a  $C_1-C_2$  bond cleavage producing a stable

353 product, acetic formic anhydride,  $\text{CH}_3\text{C}(\text{O})\text{OC}(\text{O})\text{H}$ , and  $\bullet\text{CH}_2\text{CH}_2\text{CH}_2\text{CH}_3$  radicals. Further, these  
354 radicals will react with  $\text{O}_2$  to form peroxy radicals eventually forming butyraldehyde, which was  
355 positively identified. 2) Can go through  $\alpha$ -ester rearrangement and then a C-O scission, which  
356 occurred when the H-atom abstraction is from the carbon linked to the non-carbonyl oxygen to  
357 produce a carboxylic acid and the corresponding radical coproduct. Acetic acid was identified. The  
358  $\bullet\text{C}(\text{O})(\text{CH}_2)_3\text{CH}_3$  radicals react with  $\text{O}_2$  to lead carbon dioxide and  $\bullet\text{CH}_2\text{CH}_2\text{CH}_2\text{CH}_3$  radicals. These  
359 radicals will finally form butyraldehyde.

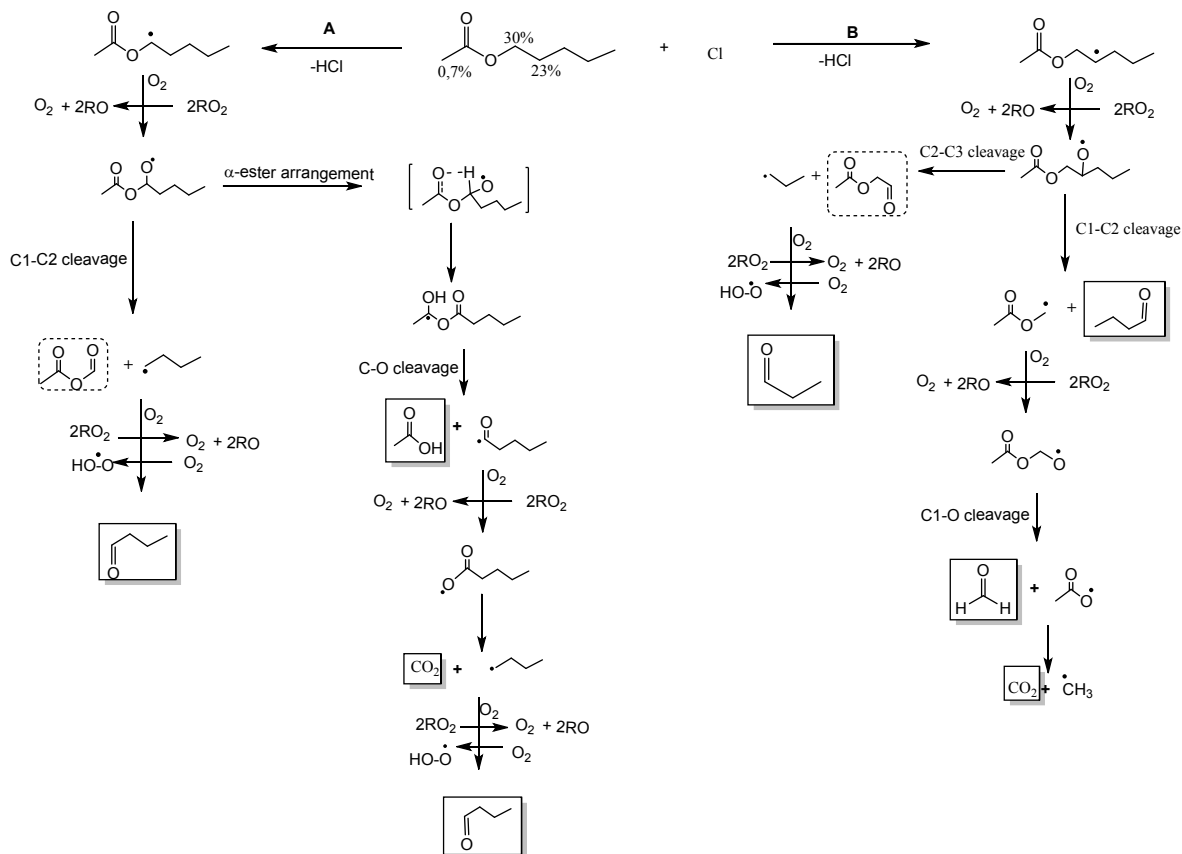
360 On the other hand, channel B shows the H-atoms abstraction from the  $-\text{CH}_2-$  ( $\text{C}_2$ ). This H abstraction  
361 generates the radical  $\text{CH}_3\text{C}(\text{O})\text{OCH}_2\text{C}(\bullet)\text{HCH}_2\text{CH}_2\text{CH}_3$  followed by  $\text{O}_2$  addition to form the peroxy  
362 radicals  $\text{CH}_3\text{C}(\text{O})\text{OCH}_2\text{C}(\text{OO}\bullet)\text{HCH}_2\text{CH}_2\text{CH}_3$  and the corresponding alkoxy radical,  
363  $\text{CH}_3\text{C}(\text{O})\text{OCH}_2\text{C}(\text{O}\bullet)\text{HCH}_2\text{CH}_2\text{CH}_3$ . These alkoxy radicals can suffer scission. If the scission occurs  
364 between  $\text{C}_1$ - $\text{C}_2$ , butyraldehyde,  $\text{CHOCH}_2\text{CH}_2\text{CH}_3$  is produced together with  $\text{CH}_3\text{C}(\text{O})\text{OC}(\bullet)\text{H}_2$   
365 radicals. These radicals react with  $\text{O}_2$  followed by  $\text{C}_1$ -O cleavage to produce formaldehyde and  $\text{CO}_2$ .  
366 In contrast, if the scission occurs between  $\text{C}_2$ - $\text{C}_3$ , 2-oxoethyl acetate,  $\text{CH}_3\text{C}(\text{O})\text{OCH}_2\text{C}(\text{O})$  is produced  
367 with  $\bullet\text{CH}_2\text{CH}_2\text{CH}_3$  radicals as coproduct. The  $\bullet\text{CH}_2\text{CH}_2\text{CH}_3$  radicals will form, propionaldehyde,  
368  $\text{CHOCH}_2\text{CH}_3$ .

369 Additionally, Scheme 2 shows two possible pathways. If the H-atoms abstraction is on the  $-\text{CH}_2-$  ( $\text{C}_3$ ),  
370 channel C, produced the radical  $\text{CH}_3\text{C}(\text{O})\text{OCH}_2\text{CH}_2\text{C}(\bullet)\text{HCH}_2\text{CH}_3$  followed by  $\text{O}_2$  addition to form  
371 the alkoxy radical  $\text{CH}_3\text{C}(\text{O})\text{OCH}_2\text{CH}_2\text{C}(\text{O}\bullet)\text{HCH}_2\text{CH}_3$ . These radicals can suffer scission. If the  
372 scission occurs between  $\text{C}_2$ - $\text{C}_3$  it is formed propionaldehyde,  $\text{CHOCH}_2\text{CH}_3$ , and  
373  $\text{CH}_3\text{C}(\text{O})\text{OCH}_2\text{C}(\bullet)\text{H}_2$  radicals. These radicals will produce formaldehyde,  $\text{CH}_2\text{O}$ , and  $\text{CO}_2$ . If the  
374 scission occurs between  $\text{C}_3$ - $\text{C}_4$  will produce the stable compound  $\text{CH}_3\text{C}(\text{O})\text{OCH}_2\text{CH}_2\text{C}(\text{O})\text{H}$ , 2-oxo-  
375 2-(3-oxopropoxy)ethan-1-ylum, and  $\bullet\text{CH}_2\text{CH}_3$  radicals. The ethyl radicals produce acetaldehyde,  
376  $\text{CHOCH}_3$ .

377 If the H-atoms abstraction is on the  $-\text{CH}_2-$  ( $\text{C}_4$ ), (channel D), will form the radical  
378  $\text{CH}_3\text{C}(\text{O})\text{OCH}_2\text{CH}_2\text{CH}_2\text{C}(\bullet)\text{HCH}_3$  followed by  $\text{O}_2$  addition to form the alkoxy radical  
379  $\text{CH}_3\text{C}(\text{O})\text{OCH}_2\text{CH}_2\text{CH}_2\text{C}(\text{O}\bullet)\text{HCH}_3$ . These radicals can undergo a cleavage between  $\text{C}_3$ - $\text{C}_4$  to lead to  
380 a stable compound, acetaldehyde,  $\text{CHOCH}_3$ , and  $\text{CH}_3\text{C}(\text{O})\text{OCH}_2\text{CH}_2\text{C}(\bullet)\text{H}_2$  radicals. These radicals  
381 could decompose to form formaldehyde and other radicals that will produce formaldehyde and  $\text{CO}_2$ .

382

383

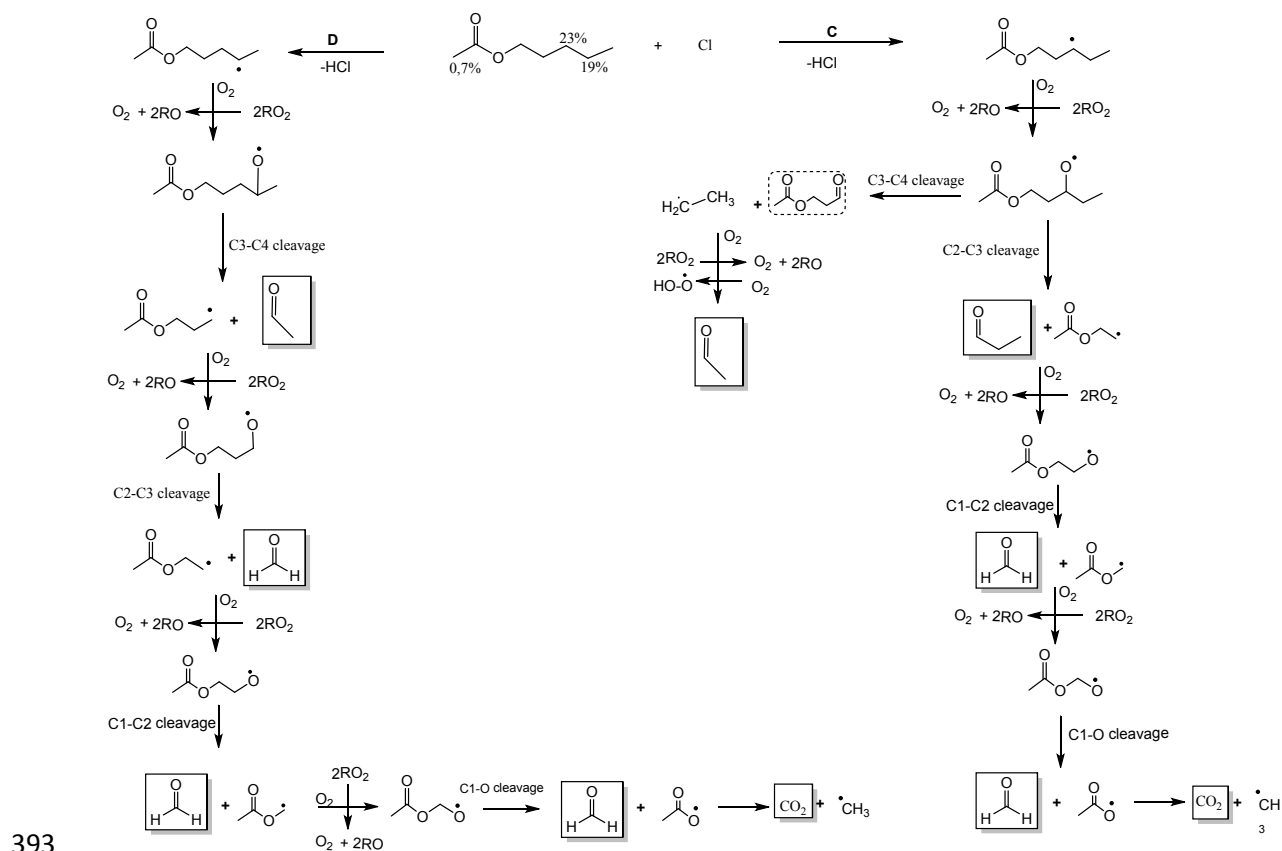


384

385 **Scheme 1.** Mechanism of Cl-atoms initiated oxidation of AA *via* H-abstraction from C<sub>1</sub> (channel A)  
 386 and C<sub>2</sub> (Channel B). Products identified in full line and unidentified products in dotted line  
 387

388 The SAR calculations predict that channel A will be the primary reaction pathway (30%), followed  
 389 by channels B and C (23%). Further studies will be necessary in order to quantify the product yields  
 390 at various conditions, such as the presence or absence of NO<sub>x</sub>, together with molecular theoretical  
 391 research, in order to fully clarify the oxidation mechanism in different atmospheric scenarios.

392



394 **Scheme 2.** Mechanism of Cl-atoms initiated oxidation of AA *via* H-abstraction from C<sub>3</sub> (channel C)  
 395 and C<sub>4</sub> (Channel D). Products identified in full line and unidentified products in dotted line  
 396

397 As far as we are aware, no previous investigations have been performed concerning the products of  
 398 AA and Cl atoms or with other tropospheric oxidants. Consequently, this is the first product  
 399 distribution analysis of the mentioned reactions. The obtained product distribution and the proposed  
 400 mechanism are consistent with the previously described pathways for the OH and Cl-initiated  
 401 degradation of other saturated esters<sup>34</sup>.

402

403

404

405

#### 406 4 Atmospheric chemistry implications

407 The rate coefficients of oxidation reactions with tropospheric oxidants such as OH radicals, Cl atoms,  
 408 O<sub>3</sub> molecules, or NO<sub>3</sub> radicals and the average tropospheric oxidant concentrations can be used to  
 409 calculate the tropospheric residence time ( $\tau$ ) by the expression  $\tau = 1/k_{AA} \times [\text{Oxidants}]$ . where [OH] is  
 410  $2.0 \times 10^6$  radicals.cm<sup>-3</sup> for about 12 hours<sup>35</sup> and [Cl] is  $(3.3 \pm 1.1) \times 10^4$  atoms.cm<sup>-3</sup> for 24 hours<sup>36</sup>

411 From Table 4, the values estimated are  $\tau_{OH} = 22$ , and  $\tau_{Cl} = 62$  hours. The short lifetime for AA in the  
 412 range of just over a few hours implies that the emission of this compound is likely to be removed  
 413 rapidly in the gas phase close to its source of emission.

414 Unfortunately, there are no kinetic data available in the literature for the reactions of this compound  
 415 with O<sub>3</sub> molecules, and NO<sub>3</sub> radicals with AA. Propyl acetate reacts with NO<sub>3</sub> with a rate coefficient  
 416 of  $(5.0 \pm 2.0) \times 10^{-17}$  cm<sup>3</sup>.molecule<sup>-1</sup>.s<sup>-1</sup> according to reported data <sup>37</sup>. It may be predicted that the rate  
 417 coefficient for AA should be on that order of magnitude with very small contribution as atmospheric  
 418 sink of this ester by reaction with NO<sub>3</sub> radicals. AA was stable to actinic radiation according to  
 419 previous photolysis investigations carried out before the kinetics experiments. These studies also did  
 420 not demonstrate a significant decrease in the signals of the FTIR.

421 **Table 4.** Atmospheric implications of AA.

422

Reaction	$k_{Average}$ cm <sup>3</sup> .molecule <sup>-1</sup> .s <sup>-1</sup>	$\tau$ h	[O <sub>3</sub> ] <sup>a</sup> ppm	POCP <sup>b</sup>
AA + OH	$(6.19 \pm 1.23) \times 10^{-12}$	22	2.15	70.2
AA + Cl	$(1.35 \pm 0.14) \times 10^{-10}$	62		

423 Reference compounds: <sup>a</sup> CH<sub>2</sub>=CH<sub>2</sub>=3.30 ppm; <sup>b</sup> CH<sub>2</sub>=CH<sub>2</sub>=100.

424 Due to the atmospheric lifetime, AA will probably contribute to ozone formation in local emission  
 425 areas. For this reason, the POCP, was estimated using the modeling technique described by Jenkin et  
 426 al., 2017, with equation 14, to evaluate the possible contribution of AA to the POCP.

$$427 \quad \text{POCP} = (A \times \gamma_S \times R \times S \times F) + P + R_{O_3} - Q \quad (14)$$

428 where, A,  $\gamma_S$ , R, and S are core parameters used for all VOCs, F, P,  $R_{O_3}$  and Q are parameters used for  
 429 specific groups of compounds, and which otherwise take default values of 1 for F or 0 for P,  $R_{O_3}$ , and  
 430 Q. The parameter A is a multiplier and  $\gamma_S$  is a variable connected to the VOC's structure.

431 With this method, the POCPs<sup>38</sup> of VOCs are calculated in relation to ethane, which is given a value  
 432 of 100. The estimated POCP value for AA is 70.2. It can be observed that, in comparison to ethane  
 433 as a reference compound, AA has significant risk of contributing to photochemical smog.  
 434 Furthermore, using the reported<sup>39</sup> Dash et al., 2013 equation (15), it was estimated the  $[O_3]$  during the  
 435 reaction of VOCs with OH radicals.

$$436 \quad O_3 = \frac{n'[k_a(OH)]^2}{4.6[2.7 \times 10^{-5} - k(OH)]} \times \left( \frac{1}{k_a(OH)} - \frac{1 - e^{-1.24 \times 10^{-4}/k_a(OH)}}{2.7 \times 10^{-5}} \right) \quad (15)$$

437 where n' is the maximum possible ozone molecules that can be produced from one molecule of VOC  
 438 based on the number of nC + nH atoms present in that molecule,  $k_a$  is the rate coefficient, and (OH)  
 439 is the global weighted-average OH radical concentration. The average ozone production during the  
 440 reaction of AA with OH radicals was estimated to be 2.15 ppm. This value can be compared with of  
 441 ethene value, 3.30 ppm. Due to the close values, the degradation of AA could have a negative impact  
 442 on human health since it will increase the tropospheric ozone.

443 The release of AA into the atmosphere can contribute to the overall chemical composition of the air.  
 444 In small quantities, it is unlikely to have a significant impact on air quality. However, if large amounts  
 445 of AA are released, either from industrial processes, it can contribute to the formation of secondary  
 446 pollutants such as ozone or particulate matter. AA can degrade in the atmosphere to produce a number  
 447 of VOCs with different impacts on the troposphere and the surface of the Planet.



448 Small aldehydes, such as formaldehyde ( $\text{CH}_2\text{O}$ ) and acetaldehyde ( $\text{CH}_3\text{CHO}$ ), can have atmospheric  
449 implications due to their reactivity. These aldehydes are highly reactive compounds in the atmosphere.  
450 They can participate in photochemical reactions, reacting with other atmospheric constituents such  
451 as hydroxyl radicals ( $\text{OH}$ ) and nitrogen oxides ( $\text{NO}_x$ )<sup>40,41</sup>. These reactions can contribute to the  
452 formation of secondary pollutants, including peroxyacyl nitrates (PANs) and ozone ( $\text{O}_3$ ), which can  
453 impact air quality. Both formaldehyde and acetaldehyde are known to contribute to the formation of  
454 ground-level ozone, which are a harmful pollutant and a component of smog. They can also contribute  
455 to the formation of secondary organic aerosols, which have implications for air quality and human  
456 health. Formaldehyde is classified as a human carcinogen by the International Agency for Research  
457 on Cancer (IARC)<sup>42</sup>, and it can cause respiratory irritation and other health issues. Acetaldehyde is a  
458 respiratory irritant and is also classified as a potential carcinogen. For this reason, numerous field  
459 studies are carried out to evaluate the levels of carbonyl VOCs as main pollutants in the atmosphere  
460 of populated cities and their potential risk to health<sup>43,44</sup>.

461 Acetic acid is readily soluble in water, and its fate in the atmosphere depends on various factors such  
462 as temperature, humidity, and reaction rates. It can undergo oxidation reactions to form other organic  
463 compounds or be scavenged by precipitation and deposited onto the Earth's surface.

## 464 **5 Conclusions**

465 Once released into the atmosphere, AA can undergo various chemical reactions. It can be degraded  
466 by reactions with hydroxyl radicals or other oxidizing agents present in the atmosphere. The exact  
467 fate of AA will depend on the specific conditions of the environment, such as the presence of sunlight,  
468 other pollutants, and the atmospheric concentrations of reactive species.

469 The residence time of AA is around 22 hours for reaction with  $\text{OH}$  radicals and 62 hours in reaction  
470 with  $\text{Cl}$  atoms. It would have a regional and local impact.

471 The degradation mechanism initiated by the Cl atoms is similar that OH radicals by H-atoms  
472 abstraction from the alkyl groups followed by O<sub>2</sub> addition to form the peroxy radicals further alkoxy  
473 radical's formation. The fate of alkoxy radicals depends on several reaction pathways.

474 AA can degrade in the atmosphere to produce a number of VOCs as acetic acid, formaldehyde,  
475 acetaldehyde, propionaldehyde, and butyraldehyde with different impacts on the troposphere. Small  
476 aldehydes can contribute to produces other pollutants, such as peroxyacyl nitrates (PANs) and ozone  
477 (O<sub>3</sub>).

478 The reaction of OH radicals with AA might have a harmful effect on human health since it will cause  
479 the creation of a considerable amount of tropospheric ozone and has a significant risk of contributing  
480 to photochemical smog.

## 481 **Conflicts of interest**

482 There are no conflicts to declare.

## 483 **Acknowledgements**

484 The authors wish to acknowledge to EUROCHAMP 2020, FONCyT, CONICET and SECyT UNC,  
485 Argentina. M. B. B. wish to acknowledge the Alexander von Humboldt Foundation for financial  
486 support. V.G.S.C wishes to acknowledge to CONICET for a doctoral fellowship and support.

## 487 **References**

- 488 1 R. Atkinson, Gas-phase tropospheric chemistry of organic compounds: a review, *Atmospheric Environment*,  
489 2007, **41**, 200–240.
- 490 2 A. El Boudali, S. Le Calvé, G. Le Bras and A. Mellouki, Kinetic Studies of OH Reactions with a Series of  
491 Acetates, *J. Phys. Chem.*, 1996, **100**, 12364–12368.
- 492 3 1: Final Report on the Safety Assessment of Amyl Acetate and Isoamyl Acetate, *Journal of the American*  
493 *College of Toxicology*, 1988, **7**, 705–719.
- 494 4 I. Barnes, K. H. Becker and N. Mihalopoulos, An FTIR product study of the photooxidation of dimethyl  
495 disulfide, *J Atmos Chem*, 1994, **18**, 267–289.
- 496 5 R. Atkinson, D. L. Baulch, R. A. Cox, R. F. Hampson, J. A. Kerr, M. J. Rossi and J. Troe, Evaluated Kinetic,  
497 Photochemical and Heterogeneous Data for Atmospheric Chemistry: Supplement V. IUPAC Subcommittee  
498 on Gas Kinetic Data Evaluation for Atmospheric Chemistry, *Journal of Physical and Chemical Reference*  
499 *Data*, 1997, **26**, 521–1011.
- 500 6 A. Bonard, V. Daële, J.-L. Delfau and C. Vovelle, Kinetics of OH Radical Reactions with Methane in the  
501 Temperature Range 295–660 K and with Dimethyl Ether and Methyl-tert-butyl Ether in the Temperature  
502 Range 295–618 K, *J. Phys. Chem. A*, 2002, **106**, 4384–4389.

- 503 7 Evaluated kinetic and photochemical data for atmospheric chemistry: Supplement IV: IUPAC subcommittee  
504 on gas kinetic data evaluation for atmospheric chemistry - ScienceDirect,  
505 <https://www.sciencedirect.com/science/article/abs/pii/S152440890300383V>, (accessed 17 March 2023).
- 506 8 E. C. Tuazon, R. Atkinson, S. M. Aschmann, M. A. Goodman and A. M. Winer, Atmospheric reactions of  
507 chloroethenes with the OH radical, *Int. J. Chem. Kinet.*, 1988, **20**, 241–265.
- 508 9 R. Atkinson and S. M. Aschmann, Kinetics of the gas-phase reactions of Cl atoms with chloroethenes at  
509  $298 \pm 2$  K and atmospheric pressure, *Int. j. chem. kinet.*, 1987, **19**, 1097–1105.
- 510 10 O. US EPA, EPI Suite™-Estimation Program Interface, [https://www.epa.gov/tsca-screening-tools/epi-](https://www.epa.gov/tsca-screening-tools/epi-suite-estimation-program-interface)  
511 [suite-estimation-program-interface](https://www.epa.gov/tsca-screening-tools/epi-suite-estimation-program-interface), (accessed 23 March 2023).
- 512 11 D. C. Williams, L. N. O'Rji and D. A. Stone, Kinetics of the reactions of OH radicals with selected acetates  
513 and other esters under simulated atmospheric conditions, *Int. J. Chem. Kinet.*, 1993, **25**, 539–548.
- 514 12 Antonia Zogka. Atmospheric degradation of a series of methoxy and ethoxy acetates and n-pentyl acetate.  
515 Other. Université d'Orléans, 2016. English. NNT : 2016ORLE2071. tel-01581321.
- 516 13 S. Ifang, T. Benter and I. Barnes, Reactions of Cl atoms with alkyl esters: kinetic, mechanism and  
517 atmospheric implications, *Environ Sci Pollut Res*, 2015, **22**, 4820–4832.
- 518 14 L. N. Farrugia, I. Bejan, S. C. Smith, D. J. Medeiros and P. W. Seakins, Revised structure activity parameters  
519 derived from new rate coefficient determinations for the reactions of chlorine atoms with a series of seven  
520 ketones at 290K and 1atm, *Chemical Physics Letters*, 2015, **640**, 87–93.
- 521 15 S. M. Aschmann and R. Atkinson, Rate constants for the gas-phase reactions of alkanes with Cl atoms at  
522  $296 \pm 2$  K: GAS-PHASE REACTIONS OF ALKANES, *Int. J. Chem. Kinet.*, 1995, **27**, 613–622.
- 523 16 J.-H. Xing, K. Takahashi, M. D. Hurley and T. J. Wallington, Kinetics of the reactions of chlorine atoms  
524 with a series of acetates, *Chemical Physics Letters*, 2009, **474**, 268–272.
- 525 17 R. Atkinson, Kinetics and mechanisms of the gas-phase reactions of the hydroxyl radical with organic  
526 compounds under atmospheric conditions, *Chem. Rev.*, 1986, **86**, 69–201.
- 527 18 G. S. Tyndall, A. S. Pimentel and J. J. Orlando, Temperature Dependence of the Alpha-Ester Rearrangement  
528 Reaction, *J. Phys. Chem. A*, 2004, **108**, 6850–6856.
- 529 19 B. Picquet, S. Heroux, A. Chebbi, J.-F. Doussin, R. Durand-Jolibois, A. Monod, H. Loirat and P. Carlier,  
530 Kinetics of the reactions of OH radicals with some oxygenated volatile organic compounds under simulated  
531 atmospheric conditions, *Int. J. Chem. Kinet.*, 1998, **30**, 839–847.
- 532 20 C. Ferrari, A. Roche, V. Jacob, P. Foster and P. Baussand, Kinetics of the reaction of OH radicals with a  
533 series of esters under simulated conditions at 295 K, *Int. J. Chem. Kinet.*, 1996, **28**, 609–614.
- 534 21 M. Veillerot, P. Foster, R. Guillermo and J. C. Galloo, Gas-phase reaction of n-butyl acetate with the  
535 hydroxyl radical under simulated tropospheric conditions: Relative rate constant and product study, *Int. J.*  
536 *Chem. Kinet.*, 1996, **28**, 235–243.
- 537 22 L. K. Christensen, J. C. Ball and T. J. Wallington, Atmospheric Oxidation Mechanism of Methyl Acetate,  
538 *J. Phys. Chem. A*, 2000, **104**, 345–351.
- 539 23 M. T. Baumgartner, R. A. Taccone, M. A. Teruel and S. I. Lane, Theoretical study of the relative reactivity  
540 of chloroethenes with atmospheric oxidants (OH, NO<sub>3</sub>, O(3P), Cl(2P) and Br(2P)), *Phys. Chem. Chem.*  
541 *Phys.*, 2002, **4**, 1028–1032.
- 542 24 M. B. Blanco, I. Bejan, I. Barnes, P. Wiesen and M. A. Teruel, Temperature-dependent rate coefficients for  
543 the reactions of Cl atoms with methyl methacrylate, methyl acrylate and butyl methacrylate at atmospheric  
544 pressure, *Atmospheric Environment*, 2009, **43**, 5996–6002.
- 545 25 N. Schütze, X. Zhong, S. Kirschbaum, I. Bejan, I. Barnes and T. Benter, Relative kinetic measurements of  
546 rate coefficients for the gas-phase reactions of Cl atoms and OH radicals with a series of methyl alkyl esters,  
547 *Atmospheric Environment*, 2010, **44**, 5407–5414.
- 548 26 S. Le Calvé, G. Le Bras and A. Mellouki, Kinetic Studies of OH Reactions with a Series of Methyl Esters,  
549 *J. Phys. Chem. A*, 1997, **101**, 9137–9141.
- 550 27 V. F. Andersen, K. B. Ørnsø, S. Jørgensen, O. J. Nielsen and M. S. Johnson, Atmospheric Chemistry of  
551 Ethyl Propionate, *J. Phys. Chem. A*, 2012, **116**, 5164–5179.
- 552 28 P. M. Cometto, V. Daële, M. Idir, S. I. Lane and A. Mellouki, Reaction Rate Coefficients of OH Radicals  
553 and Cl Atoms with Ethyl Propanoate, n -Propyl Propanoate, Methyl 2-Methylpropanoate, and Ethyl n -  
554 Butanoate, *J. Phys. Chem. A*, 2009, **113**, 10745–10752.
- 555 29 F. Taketani, Y. Matsumi, T. J. Wallington and M. D. Hurley, Kinetics of the gas phase reactions of chlorine  
556 atoms with a series of ketones, *Chemical Physics Letters*, 2006, **431**, 257–260.

- 557 30 R. Atkinson, S. M. Aschmann, W. P. L. Carter and J. N. Pitts, Rate constants for the gas-phase reaction of  
558 OH radicals with a series of ketones at  $299 \pm 2$  K: REACTION OF OH RADICALS AND KETONES, *Int.*  
559 *J. Chem. Kinet.*, 1982, **14**, 839–847.
- 560 31 E. Jiménez, B. Ballesteros, E. Martínez and J. Albaladejo, Tropospheric Reaction of OH with Selected  
561 Linear Ketones: Kinetic Studies between 228 and 405 K, *Environ. Sci. Technol.*, 2005, **39**, 814–820.
- 562 32 S. Lin and J. March, March's Advanced Organic Chemistry: Reactions, Mechanisms, and Structure, 5th  
563 Edition, *Molecules*, 2001, **6**, 1064–1065.
- 564 33 N. O. of D. and Informatics, Libro del Web de Química del NIST, <https://webbook.nist.gov/chemistry/>,  
565 (accessed 14 July 2023).
- 566 34 M. B. Blanco and M. A. Teruel, Atmospheric degradation of fluoroesters (FESs): Gas-phase reactivity study  
567 towards OH radicals at 298K, *Atmospheric Environment*, 2007, **41**, 7330–7338.
- 568 35 R. Hein, P. J. Crutzen and M. Heimann, An inverse modeling approach to investigate the global atmospheric  
569 methane cycle, *Global Biogeochemical Cycles*, 1997, **11**, 43–76.
- 570 36 O. W. Wingenter, M. K. Kubo, N. J. Blake, T. W. Smith Jr., D. R. Blake and F. S. Rowland, Hydrocarbon  
571 and halocarbon measurements as photochemical and dynamical indicators of atmospheric hydroxyl, atomic  
572 chlorine, and vertical mixing obtained during Lagrangian flights, *Journal of Geophysical Research:*  
573 *Atmospheres*, 1996, **101**, 4331–4340.
- 574 37 S. Langer, E. Ljungström and I. Wängberg, Rates of reaction between the nitrate radical and some aliphatic  
575 esters, *J. Chem. Soc., Faraday Trans.*, 1993, **89**, 425–431.
- 576 38 M. E. Jenkin, R. G. Derwent and T. J. Wallington, Photochemical ozone creation potentials for volatile  
577 organic compounds: Rationalization and estimation, *Atmospheric Environment*, 2017, **163**, 128–137.
- 578 39 M. R. Dash and B. Rajakumar, Experimental and theoretical rate coefficients for the gas phase reaction of  
579  $\beta$ -Pinene with OH radical, *Atmospheric Environment*, 2013, **79**, 161–171.
- 580 40 R. Atkinson, D. L. Baulch, R. A. Cox, J. N. Crowley, R. F. Hampson, R. G. Hynes, M. E. Jenkin, M. J.  
581 Rossi and J. Troe, Evaluated kinetic and photochemical data for atmospheric chemistry: Volume III ? gas  
582 phase reactions of inorganic halogens, *Atmospheric Chemistry and Physics*, 2007, **7**, 981–1191.
- 583 41 R. Atkinson, C. N. Plum, W. P. L. Carter, A. M. Winer and J. N. Pitts, Rate constants for the gas-phase  
584 reactions of nitrate radicals with a series of organics in air at 298 .+- . 1 K, *J. Phys. Chem.*, 1984, **88**, 1210–  
585 1215.
- 586 42 IARC, *Formaldehyde, 2-Butoxyethanol and 1-tert-Butoxypropan-2-ol. IARC Monographs on the*  
587 *Evaluation of Carcinogenic Risks to Humans Volume 88*, Lyon, France, 2006, vol. 88.
- 588 43 F. Villanueva, A. Tapia, A. Notario, J. Albaladejo and E. Martínez, Ambient levels and temporal trends of  
589 VOCs, including carbonyl compounds, and ozone at Cabañeros National Park border, Spain, *Atmospheric*  
590 *Environment*, 2014, **85**, 256–265.
- 591 44 Y.-Y. Lu, Y. Lin, H. Zhang, D. Ding, X. Sun, Q. Huang, L. Lin, Y.-J. Chen, Y.-L. Chi and S. Dong,  
592 Evaluation of Volatile Organic Compounds and Carbonyl Compounds Present in the Cabins of Newly  
593 Produced, Medium- and Large-Size Coaches in China, *Int J Environ Res Public Health*, 2016, **13**, 596.  
594

1                    **OH and Cl radicals initiated oxidation of Amyl Acetate under**  
2                    **atmospheric conditions: Kinetics, products and mechanisms**

3                    Gianni G. Straccia, C.<sup>1</sup>, María B. Blanco<sup>1,2</sup>, and Mariano A. Teruel<sup>1\*</sup>

4                    <sup>1</sup>(L.U.Q.C.A), Laboratorio Universitario de Química y Contaminación del Aire. Instituto  
5                    de Investigaciones en Fisicoquímica de Córdoba (I.N.F.I.Q.C.), Dpto. de Fisicoquímica.  
6                    Facultad de Ciencias Químicas, Universidad Nacional de Córdoba. Ciudad Universitaria,  
7                    5000 Córdoba, Argentina.

8                    <sup>2</sup> Institute for Atmospheric and Environmental Research, University of Wuppertal, DE-  
9                    42097 Wuppertal, Germany.

10                    **Fax: (+54) 351-4334188**

11                    \*e-mail: **[mariano.teruel@unc.edu.ar](mailto:mariano.teruel@unc.edu.ar)**

12

13

14

15

16

17

18

19

20

21

22

23

24

25

26

27

28

29

30            **OH and Cl radicals initiated oxidation of Amyl Acetate under**  
31            **atmospheric conditions: Kinetics, products and mechanisms.**

32            Gianni G. Straccia, C.<sup>1</sup>, María B. Blanco<sup>1,2</sup>, and Mariano A. Teruel<sup>1\*</sup>

33            <sup>1</sup>(L.U.Q.C.A), Laboratorio Universitario de Química y Contaminación del Aire. Instituto  
34            de Investigaciones en Fisicoquímica de Córdoba (I.N.F.I.Q.C.), Dpto. de Fisicoquímica.  
35            Facultad de Ciencias Químicas, Universidad Nacional de Córdoba. Ciudad Universitaria,  
36            5000 Córdoba, Argentina.

37            <sup>2</sup> Institute for Atmospheric and Environmental Research, University of Wuppertal, DE-  
38            42097 Wuppertal, Germany.

39            **Fax: (+54) 351-4334188**

40            \*e-mail: **[mariano.teruel@unc.edu.ar](mailto:mariano.teruel@unc.edu.ar)**

41

42

43

44

45

46

47

48

49

50

51

52

53

54

55

56

57

58

**59 Abstract**

60 The relative rate coefficients of the gas-phase reaction of amyl acetate, (AA),  $\text{CH}_3\text{COO}(\text{CH}_2)_4\text{CH}_3$   
61 with OH radicals and Cl atoms were determined at  $(298 \pm 2)$  K and 1000 mbar of pressure. The  
62 experiments were developed in two different atmospheric Pyrex chambers coupled with “*in situ*”  
63 Fourier Transform Infrared (FTIR) spectroscopy and Gas Chromatography equipped with flame  
64 ionization detection (GC-FID). The rate coefficients obtained from the average of different  
65 experiments were (in units of  $\text{cm}^3 \cdot \text{molecule}^{-1} \cdot \text{s}^{-1}$ ):  $k_{AA + \text{OH-FTIR}} = (6.00 \pm 0.96) \times 10^{-12}$ ;  $k_{AA + \text{OH-GC-FID}} =$   
66  $(6.37 \pm 1.50) \times 10^{-12}$  and  $k_{AA + \text{Cl-GC-FID}} = (1.35 \pm 0.14) \times 10^{-10}$ . Additionally, product studies were  
67 completed for the Cl-initiated oxidation of AA, in similar conditions of the kinetic experiments by  
68 Gas Chromatography coupled with a mass detector (GC-MS) with Solid Phase Micro Extraction  
69 (SPME). Acetic acid, formaldehyde, acetaldehyde, propionaldehyde, and butyraldehyde were the  
70 main products identified. Complementary Structure activity relationships (SAR) were developed to  
71 compare with the experimental kinetic results and to clarify the individual reactivity sites of the ester.  
72 The atmospheric oxidation pathways of the AA are postulated and discussed taking into account the  
73 observed products and the SAR estimations. The initial pathway for the degradation of AA initiated  
74 by Cl atoms and OH radicals occurs via H-atom abstraction at  $-\text{C}(\text{O})\text{OCH}_2-$  (C1);  $-\text{CH}_2-$  (C2);  $-\text{CH}_2-$   
75 (C3); and  $-\text{CH}_2\text{CH}_3-$  (C4) moieties.

76 The atmospheric implications of the reactions studied were evaluated by the estimation of their  
77 tropospheric lifetimes toward OH radicals and Cl atoms to be:  $\tau_{\text{OH}} = 22$  and  $\tau_{\text{Cl}} = 62$  hours.  
78 Consequently, the estimated average ozone production ( $[\text{O}_3] = 2.15$ ) suggests a potential contribution  
79 of these compounds emission to the formation of photochemical smog. On the other hand, the  
80 Photochemical Ozone Creation Potential (POCP) for AA was calculated to be  $\text{POCP} = 70.2$ . A  
81 moderate risk of photochemical smog production suggests that this ester could be harmful to the  
82 health and the biota in urban environments.

83 **Keywords:** Esters reactivity, SAR, GC-FID/MS, *in situ* FTIR, Free energy relationships, POCP.

## 84 **1 Introduction**

85 The atmosphere is filled with Volatile Organic Compounds (VOCs), which are released from several  
86 anthropogenic or natural sources. Numerous VOCs can undergo photochemical reactions that result  
87 in the creation of ozone and other harmful byproducts when combined with sunlight radiation and  
88 molecular oxygen. These VOCs react with hydroxyl radicals (OH), which is the main atmospheric  
89 sink and where ozone or other products are formed. Additionally, other atmospheric oxidants,  
90 including Cl atoms, NO<sub>3</sub> radicals, and O<sub>3</sub> molecules could react with these VOCs<sup>1</sup>.

91 Acetates are a type of VOCs that are extensively utilized in various industrial procedures, primarily  
92 as solvents and in the production of fragrances and flavors. In nature, vegetation also generates these  
93 substances<sup>2</sup>. AA is used as a cosmetic product, mainly in nail polishes, enamels, and lacquer.  
94 Additionally, it serves as a solvent in nail enamel remover and employed in inks, adhesives or  
95 thinners<sup>3</sup>.

96 The atmospheric oxidation of AA, which is most likely to be initiated by OH radicals or Cl atoms,  
97 may have an impact on the production of ozone and other photochemical smog byproducts in urban  
98 areas.

99 To assess the effects of anthropogenic and biological factors on air quality, it is necessary to combine  
100 kinetic data with mechanistic information about the overall oxidation process at atmospheric pressure  
101 and room temperature.

102 In the present work, we present relative rate coefficient data for the reactions of the OH radical and  
103 Cl atoms with AA at  $(298 \pm 52)$  K and 1000 mbar of pressure, using *in situ* FTIR spectroscopy and  
104 GC-FID, as analytical techniques. In addition, product studies and SAR estimations were developed  
105 for the first time for the Cl-initiated oxidation of AA to postulate the atmospheric chemical  
106 mechanism of this ester at NO<sub>x</sub> –free conditions.



107 The atmospheric lifetimes of AA were calculated using the experimental rate coefficients determined  
108 in this work to assess the potential consequences of the studied reactions on the atmosphere. The  
109 estimation of  $[O_3]$  and POCP will assess the local, regional and/or global environmental implications  
110 of the reactions studied.

## 111 **2 Experimental Section**

112 All the experiments were performed in a 405 L and 480 L Pyrex glass reactors at  $(298 \pm 2)$  K and  
113 1000 mbar = 1 atmosphere of pressure. A complete description of the reactor can be found elsewhere.<sup>4</sup>  
114 and only a brief explanation are given here. The chamber is composed of a cylindrical borosilicate  
115 glass vessel of 1.5 and 3 m. The reactors are surrounded by fluorescence lamps, which emit at a  
116 maximum of 360 nm. The radicals are produced by the radiation of the lamps. The 405 L reactor is  
117 coupled to a gas chromatograph equipped with flame ionization detection Shimadzu GC-2014B,  
118 using an Rtx-5 capillary column (fused silica G27, 30 m  $\times$  0.25 mm 0.25  $\mu$ m) using SPME as a  
119 sampling method, the gray fiber is composed of Divinylbenzene/Carboxen/Polydimethylsiloxane  
120 (DVB/CAR/PDMS).

121 On the other hand, the 480 L reactor is coupled to an *in situ* Thermo Nicolet Nexus spectrometer  
122 brand equipped with a liquid Nitrogen-Cooled Mercury-Cadmium-Telluride (MCT) detector was  
123 used to observe the loss of the reactants, and the appearance of products. This reactor has a support  
124 system for multiple reflection mirrors type "White". This system lets many reflections inside the  
125 reactor grow the optical path, which allow us to work with lower concentrations of few ppm of VOCs  
126 of interest.

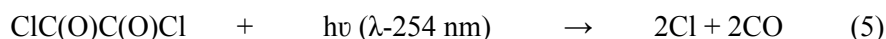
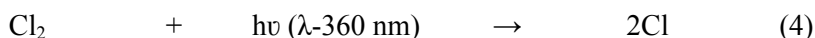
127 Using both reactors with different analytical techniques, the determination of the rate coefficients  
128 were performed by the relative method. With this method, the rate coefficient of AA could be  
129 determined indirectly from their relationship with the rate coefficient of a reference reaction.  
130 Therefore, AA and the reference compounds (ethylene, dimethyl ether, Z-1,2- dichloroethylene, and  
131 trichloroethylene) react with OH radicals or Cl atoms competitively as the following:



132 OH radicals were generated by photolysis of  $\text{H}_2\text{O}_2$  at 254 nm as follows:



133 Cl atoms were generated by UV photolysis of oxalyl chloride ( $\text{ClCOCOCl}$ ) and/or  $\text{Cl}_2$



134 Considering that reactions (1) and (2) are the only reactions that consume the reactants, it is possible

135 to determine the relative rate coefficient of the reactions of interest as:

$$136 \quad \text{Ln} \left[ \frac{[\text{AA}]_0}{[\text{AA}]_t} \right] = \frac{k_{\text{AA}}}{k_{\text{Ref}}} \text{Ln} \left[ \frac{[\text{Ref}]_0}{[\text{Ref}]_t} \right] \quad (6)$$

137 where  $[\text{Ref}]_0$ ,  $[\text{Ref}]_t$ ,  $[\text{AA}]_0$ , and  $[\text{AA}]_t$  are the concentrations of the reference compound and AA at  
 138 times  $t = 0$  and  $t$ , respectively. The slope of plots of equation 6 is the relationship between the rate  
 139 coefficient of the reference compound and AA.

140 Previous tests were carried out to check that reactions (1) and (2) were the only ones that occur  
 141 significantly inside the reactor. To ensure any reactions between them, the tests involved combining  
 142 specified quantities of AA with various reference compounds. These mixtures were then exposed to  
 143 the lamps to check the photolysis of the compound. Furthermore, no reactions between the  
 144 compounds and radical's precursor in the dark were detected.

145 For product studies, mixtures of AA with oxidants in synthetic air/N<sub>2</sub> were irradiated; in a similar  
146 condition as in the kinetic study. We used GC-MS to identify the products reaction. In addition, the  
147 products were monitored with a GC-MS VARIAN Saturn 2200 with column HP-5MS, Agilent (Part  
148 19091S-433) of 30 meters in length, 0.25 mm internal diameter and film thickness 0.25 μm. The  
149 following sampling techniques were used to take gas samples from the chamber: a) the SPME was  
150 treated to derivatization using O-((perfluorobenzyl) methyl) hydroxylamine (PFBHA). For this, the  
151 microfiber was exposed for 2 minutes for headspace extraction to the derivatizing agent solution.  
152 After the SPME covered with PFBHA was exposed to the chamber with the gas reaction for 5 minutes  
153 before being injected into the GC-MS at 220 °C. b) The SPME was exposed for 10 minutes to the gas  
154 reaction by the pre-concentration method followed by the injection into the GC-MS for 2 minutes at  
155 180 °C.

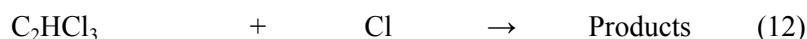
156 The initial concentrations (in ppm) used in the experiments were for AA (3) by FTIR and (6) by GC-  
157 FID, (2.4) for ethylene, (2.4) for dimethyl ether, (8) for Z-1,2- dichloroethylene, (7) for  
158 trichloroethylene, (77) for hydrogen peroxide. (1 ppm =  $2.46 \times 10^{13}$  molecule.cm<sup>-3</sup> at 298 K and 760  
159 Torr of total pressure).

160 The chemicals used in the experiments had the following purities as given by the manufacturer and  
161 were used as supplied: nitrogen (Air Liquid 99.999 %), synthetic air (Air Liquid, 99.999 %), Cl<sub>2</sub>  
162 (Messer Griesheim, 2.8), amyl acetate (Sigma-Aldrich, ≥99 %), ethylene (Sigma-Aldrich, ≥99.5%),  
163 dimethyl ether (Sigma-Aldrich, 99%), Z-1,2- dichloroethylene (Sigma-Aldrich, 97%),  
164 trichloroethylene (Supelco, 98%), and hydrogen peroxide (Interox, 85% w/w ).

## 165 **3 Results and discussion**

### 166 **3.1 Kinetics**

167 The rate coefficients for the reactions studied (1) and (2) were determined employing equation (6)  
168 with different reference compounds for each technique as follows:



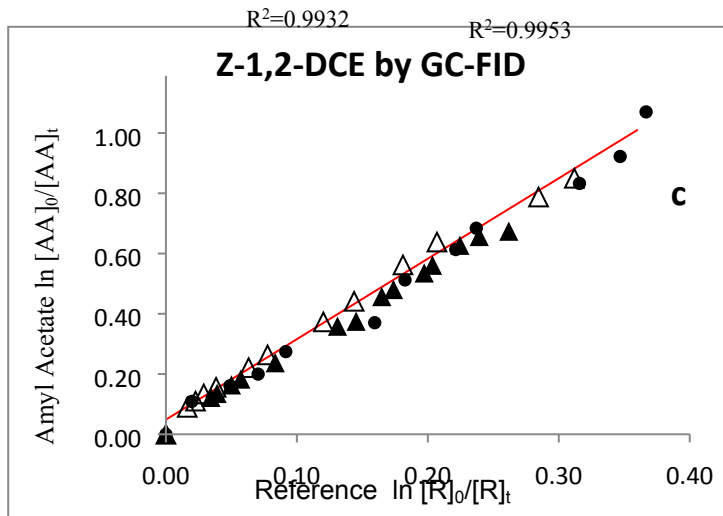
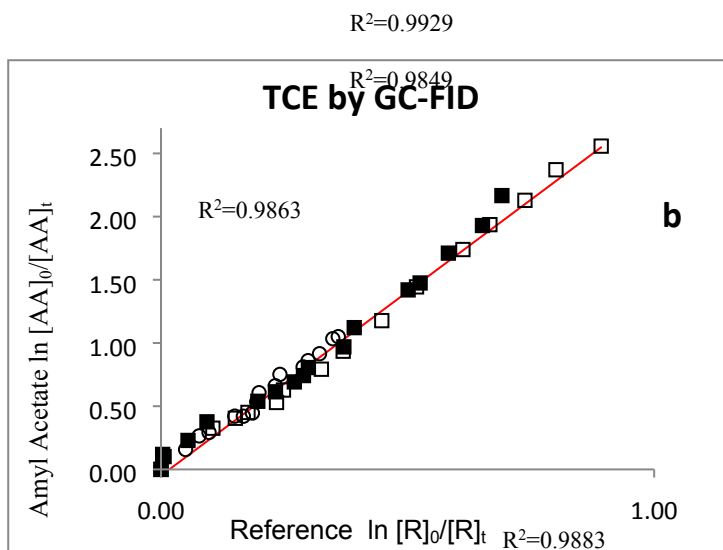
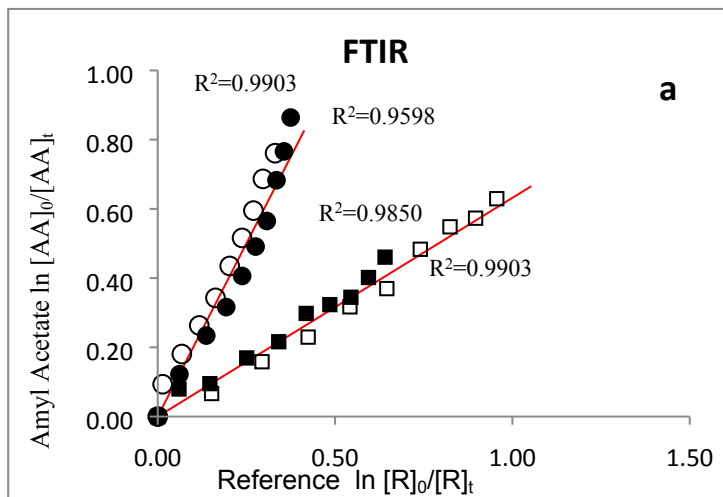
169 where  $k_7^5 = (9.00 \pm 0.30) \times 10^{-12}$ ;  $k_8^6 = (2.77 \pm 0.07) \times 10^{-12}$ ;  $k_9^7 = (2.23 \pm 0.10) \times 10^{-12}$ ;  $k_{10}^8 = (2.38 \pm$   
 170  $0.14) \times 10^{-12}$ ;  $k_{11}^9 = (9.65 \pm 0.10) \times 10^{-11}$ ;  $k_{12}^9 = (8.08 \pm 0.10) \times 10^{-11}$ . All the  $k$  values are in units of  
 171  $\text{cm}^3 \cdot \text{molecule}^{-1} \cdot \text{s}^{-1}$ .

172 The rate coefficients for the reaction under study with two oxidants were determined by the  
 173 performance of at least two experiments. Figures 1a, 1b and 1c show the plots  $\ln[\text{AA}]_0/[\text{AA}]_t$  versus  
 174  $\ln[\text{Reference}]_0/\text{Reference}]_t$  of two or three samples for each reference compound for the OH initiated  
 175 reactions. **1a** Shows the plots obtained by the FTIR technique developed using  $\text{N}_2$  with ethene and  
 176 dimethyl ether as reference compounds. **1b** and **1c** shows the plots obtained by the GC-FID technique  
 177 using synthetic air as a gas bath with trichloroethylene and Z-1,2- dichloroethylene as reference  
 178 compounds, respectively.

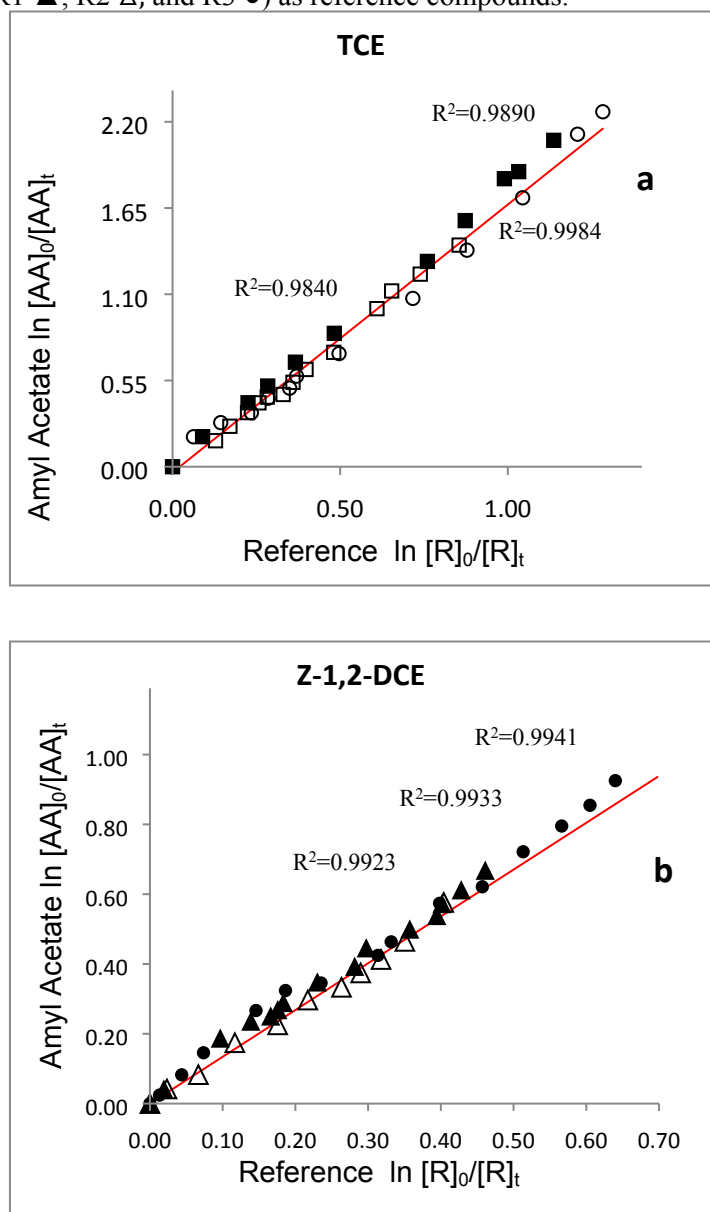
179 All plots show linearity of the straight lines obtained, with correlation coefficients close to 1 and  
 180 nearly zero intercepts indicating that secondary reactions are negligible.

181 Figure 2 shows plots obtained for the reaction of AA with Cl atoms. **2a** shows the plots of three  
 182 experiments performed using trichloroethylene as reference compounds and **2b** shows the plots  
 183 obtained using Z-1,2- dichloroethylene as reference compounds.

184



186 **Figure 1.** Kinetic data for the reaction of AA with OH radicals obtained at 298 K and atmospheric  
 187 pressure with (a) FTIR technique using ethene (R1 □ and R2 ■) and dimethyl ether (R1 ○ and R2 ●)  
 188 and (b) GC-FID technique using trichloroethylene (R1 □, R2 ■, and R3 ○) and (c) Z-1,2-  
 189 dichloroethylene (R1 ▲, R2 △, and R3 ●) as reference compounds.



190

191 **Figure 2.** Kinetic data for the reaction of AA with (ClC(O)C(O)Cl) as precursor of Cl atoms obtained  
 192 at 298 K and atmospheric pressure with GC-FID technique using (a) trichloroethylene (R1 □, R2 ■,  
 193 and R3 ○) and (b) Z-1,2- dichloroethylene (R1 ▲, R2 △, and R3 ●) as reference compounds  
 194  
 195

196 Table 1 lists the rate coefficients for the reaction of each reference compound with both oxidants. It  
 197 also includes the ( $k_{AA}/k_{reference}$ ) ratios obtained from measurements conducted using both oxidants and  
 198 techniques, along with the corresponding rate coefficient values in absolute terms. These rate  
 199 coefficient ratios are each from the average of two or three measurements. The value of the photolysis  
 200 rate for AA is also included. This value was used to correct the final value of the rate coefficient for  
 201 each reaction.

202  
 203 **Table 1.** Rate coefficient ratios  $k_{AA}/k_{reference}$ ,  $k_{photolysis}$ , rate coefficients for the reactions of OH radicals  
 204 and Cl atoms with AA using different reference compounds at  $(298 \pm 2)$  K in 760 Torr of pressure  
 205

	$k_{photolysis}$ $_{AA} \times s^{-1}$	Technique	Reference compound	$k_{reference}$ $\times 10^{12}$	$k_{AA}/$ $k_{reference}$	$k_{AA} \times 10^{12}$ $cm^3.molecul$ $e^{-1}.s^{-1}$
AA + OH	$5.29 \times 10^{-5}$	FTIR	C <sub>2</sub> H <sub>4</sub>	$9.00 \pm 0.30$	$0.66 \pm 0.04$	$5.94 \pm 0.55$
					$0.68 \pm 0.02$	$6.12 \pm 0.39$
			C <sub>2</sub> H <sub>6</sub> O	$2.77 \pm 0.07$	$2.15 \pm 0.16$	$5.96 \pm 0.59$
					$2.16 \pm 0.07$	$5.98 \pm 0.34$
			<b>Average</b>			<b><math>6.00 \pm 0.96</math></b>
	$2.42 \times 10^{-3}$	GC-FID			$2.90 \pm 0.18$	$6.47 \pm 0.69$
			C <sub>2</sub> HCl <sub>3</sub>	$2.23 \pm 0.10$	$2.91 \pm 0.14$	$6.49 \pm 0.60$
					$2.89 \pm 0.09$	$6.44 \pm 0.49$
			Z-C <sub>2</sub> H <sub>2</sub> Cl <sub>2</sub>	$2.38 \pm 0.14$	$2.59 \pm 0.10$	$6.16 \pm 0.60$
					$2.67 \pm 0.14$	$6.36 \pm 0.70$
			$2.65 \pm 0.11$	$6.31 \pm 0.63$		
		<b>Average</b>			<b><math>6.37 \pm 1.50</math></b>	
	$k_{photolysis}$ $_{AA} \times s^{-1}$	Technique	Reference compound	$k_{reference}$ $\times 10^{11}$	$k_{AA}/$ $k_{reference}$	$k_{AA} \times 10^{10}$ $cm^3.molecul$ $e^{-1}.s^{-1}$
AA + Cl	$2.27 \times 10^{-3}$	GC-FID			$1.82 \pm 0.02$	$1.47 \pm 0.03$
			C <sub>2</sub> HCl <sub>3</sub>	$8.08 \pm 0.10$	$1.63 \pm 0.06$	$1.32 \pm 0.07$
					$1.71 \pm 0.05$	$1.38 \pm 0.06$
					$1.36 \pm 0.06$	$1.31 \pm 0.07$
			Z-C <sub>2</sub> H <sub>2</sub> Cl <sub>2</sub>	$9.65 \pm 0.10$	$1.34 \pm 0.04$	$1.28 \pm 0.05$
					$1.37 \pm 0.05$	$1.32 \pm 0.06$
		<b>Average</b>			<b><math>1.35 \pm 0.14</math></b>	

206 Table 1 shows that there is good agreement between the results obtained using two different  
207 simulation chambers, four different reference compounds and *in situ* FTIR and GC-FID as detection  
208 methods. The following are the recommended average rate coefficients:

209 
$$k_{AA+OH-FTIR} = (6.00 \pm 0.96) \times 10^{-12} \text{ cm}^3 \cdot \text{molecule}^{-1} \cdot \text{s}^{-1}$$

210 
$$k_{AA+OH-GC-FID} = (6.37 \pm 1.50) \times 10^{-12} \text{ cm}^3 \cdot \text{molecule}^{-1} \cdot \text{s}^{-1}$$

211 
$$k_{AA+Cl-GC-FID} = (1.35 \pm 0.14) \times 10^{-10} \text{ cm}^3 \cdot \text{molecule}^{-1} \cdot \text{s}^{-1}$$

212 The errors shown are twice the standard deviation that results from the least-squares fit of the straight  
213 lines. The corresponding error has also been considered in the reference rate coefficients of the  
214 reaction.

215 The values of the rate coefficients of reactions with OH radicals are found to be fairly similar between  
216 2 different detection techniques, *in situ* infrared spectroscopy and gas chromatography with sample  
217 extraction by SPME.

218 For comparison purposes, the rate coefficient for the reaction of AA with OH radicals was estimated  
219 from the Structure-Activity Relationships (SAR). The rate coefficient calculation software (US  
220 Environmental Protection Agency), AOPWIN v.4.11 was used, based on the method developed by  
221 Kwok and Atkinson (1995)<sup>10</sup>. The rate coefficient calculated for H-abstraction was  $6.02 \times 10^{-12}$   
222  $\text{cm}^3 \cdot \text{molecule}^{-1} \cdot \text{s}^{-1}$ . It is shown a good concordance between the estimated rate coefficients values by  
223 SAR calculations and the obtained experimentally by FTIR  $(6.00 \pm 0.96) \times 10^{-12} \text{ cm}^3 \cdot \text{molecule}^{-1} \cdot \text{s}^{-1}$  and  
224 by GC-FID  $(6.37 \pm 1.50) \times 10^{-12} \text{ cm}^3 \cdot \text{molecule}^{-1} \cdot \text{s}^{-1}$ .



225 Furthermore, there are previous kinetic data reported for the reactions of OH radicals with AA,  
 226 performed with pulsed Laser Photolysis Laser Induced Fluorescence technique (PLP-LIF), where it  
 227 can be possible to compare with our relative determination in atmospheric conditions. The authors  
 228 reported the absolute value<sup>2</sup> of  $(7.34 \pm 0.91) \times 10^{-12} \text{ cm}^3 \cdot \text{molecule}^{-1} \cdot \text{s}^{-1}$ . On the other hand, Williams et  
 229 al. 1993, reported relative values for the rate coefficient of AA with OH radicals using Gas  
 230 Chromatography with Flame Ionization Detection<sup>11</sup> of:  $(7.53 \pm 0.48) \times 10^{-12} \text{ cm}^3 \cdot \text{molecule}^{-1} \cdot \text{s}^{-1}$ .  
 231 Additionally, previous kinetic study of AA with OH radicals reaction are reported in a doctoral  
 232 theses<sup>12</sup> by Zogka, 2016. In that theses, values of  $k_{\text{AA}+\text{OH}+1,3\text{-dioxolane}} = (6.96 \pm 0.27) \times 10^{-12} \text{ cm}^3 \cdot \text{molecule}^{-1} \cdot \text{s}^{-1}$   
 233  $^1 \cdot \text{s}^{-1}$  and  $k_{\text{AA}+\text{OH}+1\text{-pentanol}} = (7.61 \pm 0.33) \times 10^{-12} \text{ cm}^3 \cdot \text{molecule}^{-1} \cdot \text{s}^{-1}$ , were determined using relative  
 234 technique and atmospheric simulation chamber of Teflon coupled to GC-FID. Although, there are  
 235 small differences within the experimental errors, the agreement between the data obtained in this  
 236 work by GC-FID and by *in situ* FTIR with the previous relative GC-FID and PLP-LIF values is  
 237 reasonable, taking into account the experimental errors of all determinations.

238 Additionally, the predicted rate coefficient for the reaction of AA with Cl atoms was also evaluated  
 239 using the SAR method. This method was first developed to study how alkanes react with Cl atoms,  
 240 but it has been modified to take additional functional groups in more complex compounds into  
 241 account<sup>13</sup>. This method consists of computing the overall rate coefficient based on the estimation of  
 242 the rate coefficient for H-abstraction atoms from the groups  $-\text{CH}_3$ ,  $-\text{CH}_2-$  and  $>\text{CH}-$  for the  
 243 interaction of Cl atoms with alkanes<sup>14</sup>.

244 The group rate coefficients just consider the identity of the substituents next to the alkyl moiety as  
 245 follow:

$$246 \quad k(\text{CH}_3\text{-X}) = k_{\text{prim}} F(X),$$

$$247 \quad k(\text{X-CH}_2\text{-Y}) = k_{\text{sec}} F(X) F(Y),$$

$$248 \quad k(\text{X-CH-Y(Z)}) = k_{\text{tert}} F(X) F(Y) F(Z)$$

249 where,  $k_{prim} = 3.32$ ,  $k_{sec} = 8.34$ ,  $k_{tert} = 6.09$  all  $k$  in unit of ( $\times 10^{-11}$   $\text{cm}^3 \cdot \text{molecule}^{-1} \cdot \text{s}^{-1}$ ).  $F(X)$   $F(Y)$   $F(Z)$   
 250 are the moieties factor of the substituent groups  $X$ ,  $Y$ , and  $Z$ , respectively<sup>15</sup>. The SAR values were  
 251 calculated using the available substituent factors reported in many studies. Table 2 presents the factor  
 252 for each moiety compiled according to the structure of the AA,  $\text{CH}_3\text{COO}(\text{CH}_2)_4\text{CH}_3$ .

253

254

255

**Table 2.** SAR group reactivity factors for the reaction with Cl atoms.

Substituent	Factor <sub>(Cl)</sub>	Reference
(-C(O)OR)	0.12	Ifang et al, 2015 <sup>13</sup>
(RC(O)O-)	0.066	Xing et al, 2009 <sup>16</sup>
(-CH <sub>3</sub> )	1	Aschmann and Atkinson <sup>15</sup>
(-CH <sub>2</sub> -)	0.79	

256 From the data presented in Table 2 the following SAR value for the reaction of AA with Cl atoms  
 257 has been estimated:  $2.05 \times 10^{-10}$   $\text{cm}^3 \cdot \text{molecule}^{-1} \cdot \text{s}^{-1}$ . It should be observed that the estimated rate  
 258 coefficients value and the experimentally measured of  $(1.35 \pm 0.14) \times 10^{-10}$   $\text{cm}^3 \cdot \text{molecule}^{-1} \cdot \text{s}^{-1}$  are close  
 259 considering the experimental error.

260 Moreover, there are previous kinetic data reported by Zogka, 2016<sup>12</sup> for the reactions of AA with Cl  
 261 atoms. Values reported were  $k_{\text{AA}+\text{Cl}+\text{n-pentane}} = (2.07 \pm 0.04) \times 10^{-10}$   $\text{cm}^3 \cdot \text{molecule}^{-1} \cdot \text{s}^{-1}$  and  $k_{\text{AA}+\text{Cl}+\text{1-butanol}} =$   
 262  $(2.13 \pm 0.03) \times 10^{-10}$   $\text{cm}^3 \cdot \text{molecule}^{-1} \cdot \text{s}^{-1}$ . The values reported by us could be slightly lower than those  
 263 reported by Zogka. However, there is another value reported by Ifang et al. 2015. The rate coefficient  
 264 informed<sup>13</sup> of  $(1.790 \pm 0.153) \times 10^{-10}$   $\text{cm}^3 \cdot \text{molecule}^{-1} \cdot \text{s}^{-1}$  is also in agreement with the value reported in  
 265 this work.

266

267 A previous reaction trend reported by Atkinson 1986<sup>17</sup> for acetates pointed out that the rate coefficient  
 268 for the reaction of acetates with OH radicals increases with the length of the carbon chain. The  
 269 following rate coefficient values have been reported in several studies:  $\text{CH}_3\text{C}(\text{O})\text{OCH}_3$ ,  $k_{(\text{methyl acetate} + \text{OH})}^{18} = 3.5 \times 10^{-13}$ ;  
 270  $\text{CH}_3\text{C}(\text{O})\text{OCH}_2\text{CH}_3$ ,  $k_{(\text{ethyl acetate} + \text{OH})}^{19} = 1.73 \times 10^{-12}$ ;  $\text{CH}_3\text{C}(\text{O})\text{OCH}_2\text{CH}_2\text{CH}_3$ ,  $k_{(\text{propyl acetate} + \text{OH})}^{20} = 1.97 \times 10^{-12}$ ;  
 271  $\text{CH}_3\text{C}(\text{O})\text{OCH}_2\text{CH}_2\text{CH}_2\text{CH}_3$ ,  $k_{(\text{butyl acetate} + \text{OH})}^{21} = 5.20 \times 10^{-12}$ ;  
 272  $\text{CH}_3\text{C}(\text{O})\text{OCH}_2\text{CH}_2\text{CH}_2\text{CH}_2\text{CH}_3$ ,  $k_{(\text{AA} + \text{OH})\text{-Average this work}} = 6.19 \times 10^{-12}$ . All the  $k$  values are in units of  
 273  $\text{cm}^3 \cdot \text{molecule}^{-1} \cdot \text{s}^{-1}$ . That is the  $k_{\text{OH}}$  increase with the number of secondary ( $\text{CH}_2$ ) and tertiary ( $\text{C-H}$ )  
 274 bonds. On the other hand, there is a similar trend for the reactions of acetates with Cl atoms. Several  
 275 research have reported the corresponding rate coefficient values for the Cl atoms as follows:  
 276  $\text{CH}_3\text{C}(\text{O})\text{OCH}_3$ ,  $k_{(\text{methyl acetate} + \text{Cl})}^{22} = 2.20 \times 10^{-12}$ ;  $\text{CH}_3\text{C}(\text{O})\text{OCH}_2\text{CH}_3$ ,  $k_{(\text{ethyl acetate} + \text{Cl})}^{13} = 1.71 \times 10^{-11}$ ;  
 277  $\text{CH}_3\text{C}(\text{O})\text{OCH}_2\text{CH}_2\text{CH}_3$ ,  $k_{(\text{propyl acetate} + \text{Cl})}^{13} = 7.70 \times 10^{-11}$ ;  $\text{CH}_3\text{C}(\text{O})\text{OCH}_2\text{CH}_2\text{CH}_2\text{CH}_3$ ,  $k_{(\text{butyl acetate} + \text{Cl})}^{13} =$   
 278  $1.20 \times 10^{-10}$ ;  $\text{CH}_3\text{C}(\text{O})\text{OCH}_2\text{CH}_2\text{CH}_2\text{CH}_2\text{CH}_3$ ,  $k_{(\text{AA} + \text{Cl})\text{-Average this work}} = 1.35 \times 10^{-10}$ . Similar to the reaction  
 279 with OH radicals, the rate coefficient for the reaction of acetates with Cl atoms increases with the  
 280 length of the carbon chain. The values obtained in this work are consistent with the trend reported.  
 281 There is the first experimental kinetic study of the reaction of AA with Cl atoms using the relative  
 282 kinetic technique in a photoreactor coupled to FTIR spectrometers<sup>13</sup>.

### 283 3.2 Free energy relationships

284 Several studies found a linear relationship between the rate coefficients of different compounds in  
 285 reaction with OH radicals and Cl atoms<sup>23,24</sup>. In this study, Table 3 shows a relationship between  $k_{\text{OH}}$   
 286 and  $k_{\text{Cl}}$  of several acetates and ketones reported previously in the literature, including the kinetic data  
 287 for AA from the present determination. The relationship between the rate coefficients for the  
 288 reactions of OH radicals and Cl atoms is presented in Figure 3 where a significant correlation is  
 289 established. The data from Figure 3 are subjected to a least-squares analysis, which produces the  
 290 following expression:

$$\log k_{\text{OH}} = 1.1294 \log k_{\text{Cl}} - 0.0123 \quad (r^2 = 0.99) \quad (13)$$

**Table 3.** Comparison between  $k_{\text{OH}}$  and  $k_{\text{Cl}}$  of a series of acetates and ketones, together with the kinetic data for AA obtained in this work, at  $(296 \pm 2)$  K.

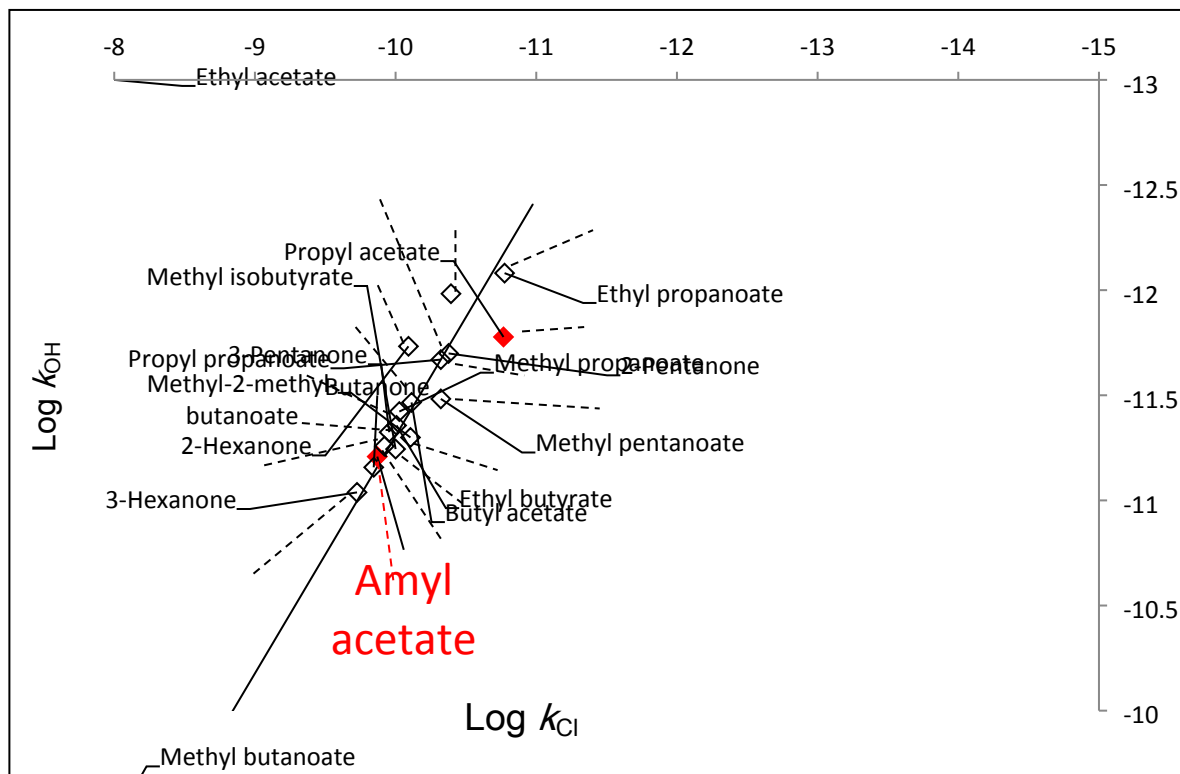
Compound	$k_{\text{Cl}}$	Ref Cl	$k_{\text{OH}}$	Ref OH
Methyl acetate	$2.20 \times 10^{-12}$	22	$3.20 \times 10^{-13}$	2
Ethyl acetate	$1.71 \times 10^{-11}$	13	$1.67 \times 10^{-12}$	2
Propyl acetate	$7.70 \times 10^{-11}$	13	$3.42 \times 10^{-12}$	2
Butyl acetate	$1.20 \times 10^{-10}$	13	$5.52 \times 10^{-12}$	2
Amyl acetate	$1.35 \times 10^{-10}$	This work	$6.19 \times 10^{-12}$	This work
Methyl butanoate	$4.77 \times 10^{-11}$	25	$3.29 \times 10^{-12}$	25
Methyl pentanoate	$7.84 \times 10^{-11}$	25	$5.02 \times 10^{-12}$	25
Methyl-2-methyl- butanoate	$9.41 \times 10^{-11}$	25	$3.78 \times 10^{-12}$	25
Methyl propanoate	$1.68 \times 10^{-11}$	13	$8.30 \times 10^{-13}$	26
Ethyl propanoate	$4.19 \times 10^{-11}$	13	$2.14 \times 10^{-12}$	27
Propyl propanoate	$9.84 \times 10^{-11}$	13	$4.40 \times 10^{-12}$	28
Ethyl butyrate	$1.00 \times 10^{-10}$	28	$5.70 \times 10^{-12}$	28
Methyl isobutyrate	$4.20 \times 10^{-11}$	28	$2.00 \times 10^{-12}$	28
2-pentanone	$1.11 \times 10^{-10}$	29	$4.74 \times 10^{-12}$	30
3-pentanone	$8.10 \times 10^{-11}$	29	$1.85 \times 10^{-12}$	30
2-hexanone	$1.88 \times 10^{-10}$	29	$9.16 \times 10^{-12}$	30
3-hexanone	$1.43 \times 10^{-10}$	29	$6.96 \times 10^{-12}$	30
Butanone	$4.04 \times 10^{-11}$	29	$1.04 \times 10^{-12}$	31

295

296 There is a direct relationship between the rate coefficients for both oxidants as it can be seen in the  
297 free energy plot for the various oxygenated compounds.

298 The good quality of the correlation between the reaction rate coefficients of OH radicals and Cl atoms  
299 is such that an estimation of the rate coefficients can be made for reactions which have not yet been  
300 investigated. In addition, this correlation shows that the degradation mechanism initiated by the Cl  
301 atoms is similar that OH radicals, *i.e.*, by the abstraction of the H atoms.

302



303

304 **Figure 3:** Free energy plots  $\log(k_{OH})$  vs.  $\log(k_{Cl})$  for the reactions with Cl and OH of acetates  
 305 and ketones reported in previous work together with the AA studied in this work (Table 3).

306

### 307 3.3. Products studies

308 Mixtures of AA with molecular chlorine in air were photolyzed to identify the oxidation products.

309 These experiments were conducted under similar conditions to the kinetic experiments.

310 Approximately 50% of consumption the original ester concentration was used in the development of

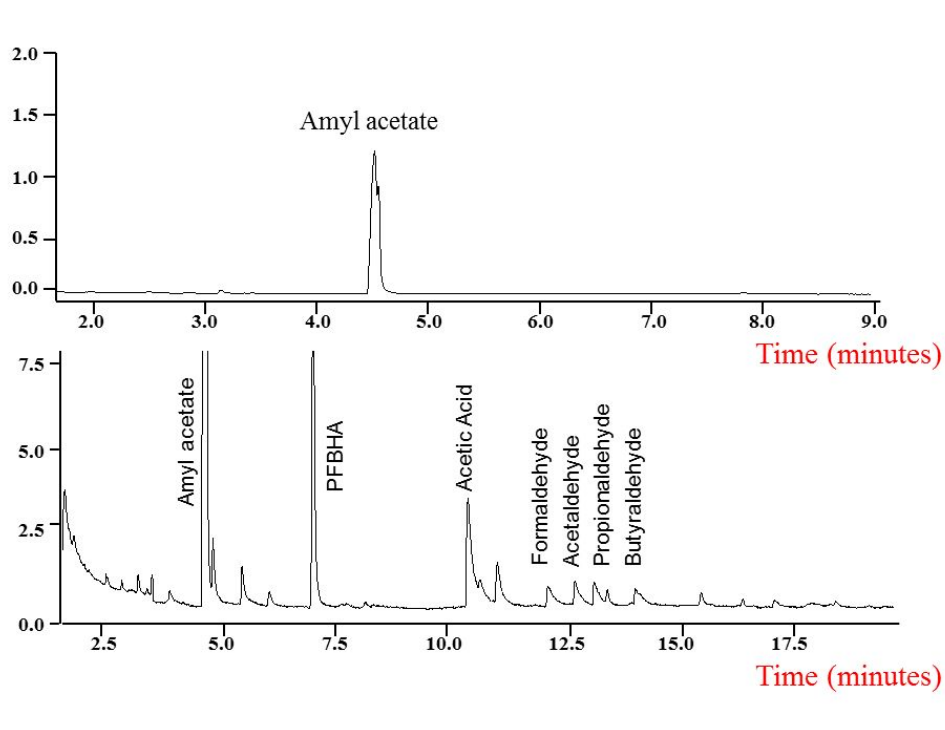
311 each study.

312 The atmospheric degradation of saturated esters with atmospheric oxidants is initiated by H-atoms  
313 abstraction from the alkyl groups CH; CH<sub>2</sub>; and/or CH<sub>3</sub>. This produces alkyl radicals with the  
314 following stability trend<sup>32</sup> being CH>CH<sub>2</sub>>CH<sub>3</sub>. The abstraction of H-atoms will be based on SAR  
315 estimated probability as follows; 0.7% at -CH<sub>3</sub>C(O)O-; 30% at -C(O)OCH<sub>2</sub>- (C1); 23% at -CH<sub>2</sub>-  
316 (C2); 23% at -CH<sub>2</sub>- (C3); 19% at -CH<sub>2</sub>CH<sub>3</sub>- (C4); and 3% at -CH<sub>3</sub> (C5);. These probabilities obtained  
317 from SAR estimation proposed that there will be several routes and secondary carbons will be the  
318 main pathway of H-atom abstraction.

319 GC-MS studies were developed to identify the end products of the chemical reaction between AA  
320 and Cl atoms. The SPME (DVB/CAR/PDMS) microfiber was exposed in the PFBHA before being  
321 exposed to the gas reaction in the Pyrex chamber. The products, formaldehyde, acetaldehyde,  
322 propionaldehyde, and butyraldehyde were positively identified as carbonyl oximes due to the reaction  
323 with the PFBHA (See Figures 4 and 5). The following carbonyl oximes were found: formaldehyde  
324 oxime, o-[(pentafluorobenzyl) methyl]; acetaldehyde oxime, o-[(pentafluorobenzyl) methyl];  
325 propionaldehyde oxime, o-[(pentafluorobenzyl) methyl]; and butyraldehyde oxime, o-  
326 [(perfluorobenzyl) methyl]. Acetic acid was found without derivatizing on the experiments by the  
327 pre-concentration method.

328 The mixture was photolyzed using air as bath gas and AA was detected at a retention time of 4.6 min  
329 with the matching ( $m/z$ ) ratios of 43, 55, 70, 87 and 115 (see Figures 4 and 5). The particular fragments  
330 ( $m/z$ ) of the main products at the successive retention times and the percentage of coincidence (match)  
331 are also shown in Figure 4: formaldehyde at 11.7 min, ( $m/z$ ): 47, 61, 81, 99, 117, 131, 161, 167, 181,  
332 and 225, with a match=97%; acetaldehyde at 12.9 min, ( $m/z$ ): 58, 81, 99, 117, 131, 161, 167, 181,  
333 209, and 239, with a match=90%; propionaldehyde at 13.2 min, ( $m/z$ ): 44, 54, 72, 99, 117, 131, 161,  
334 167, 181, 203, 236, and 253, with a match=95%; butyraldehyde at 14 min, ( $m/z$ ): 41, 55, 69, 86, 117,  
335 131, 161, 167, 181, 207, 222, 239, and 267, with a match=92%; and acetic acid at 10.3 min, ( $m/z$ ):  
336 29, 36, 40, 43, 45, 56, 60, and 61, with a match=92%. All of these fragments  $m/z$  are characteristic of  
337 these identified compounds<sup>33</sup>.

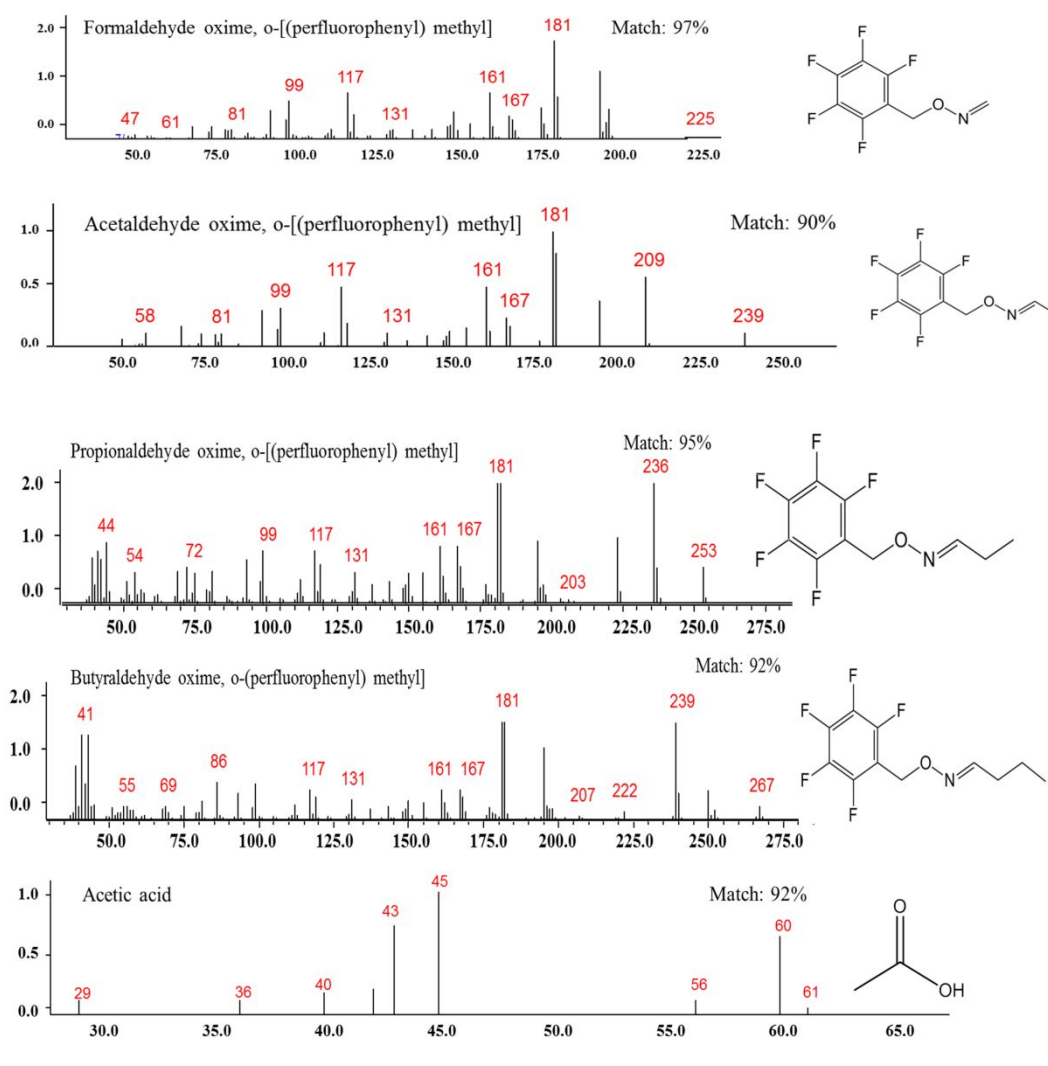
338 We postulate a degradation mechanism in Schemes 1 and 2 with four potential pathways, taking into  
339 account the products found and the SAR estimations of the reactive sites of AA.



340

341 **Figure 4.** GC-MS chromatogram of mixture of (AA + Cl<sub>2</sub>) on air, before and after photolysis.

342



343

344 **Figure 5.** Products observed and the mass spectra for formaldehyde,  
 345 propionaldehyde, butyraldehyde and acetic acid.

346 Scheme 1 shows that the reaction between Cl atoms and AA can occur via H-atom abstraction at the  
 347  $-C(O)OCH_2-$ , ( $C_1$ ), in channel A and from  $-CH_2-$  ( $C_2$ ) in channel B.

348 From channel A, the H-atoms abstraction from  $C_1$  produces the alkyl radical  
 349  $CH_3C(O)OC(\bullet)H(CH_2)_3CH_3$  followed by  $O_2$  addition to form the peroxy radicals  
 350  $CH_3C(O)OC(OO\bullet)H(CH_2)_3CH_3$  with further alkoxy radicals formation  
 351  $(CH_3C(O)OC(O\bullet)H(CH_2)_3CH_3)$ . These  $CH_3C(O)OC(O\bullet)H(CH_2)_3CH_3$  radicals can follow two  
 352 different reaction pathways: 1) decomposition, with a  $C_1-C_2$  bond cleavage producing a stable



353 product, acetic formic anhydride,  $\text{CH}_3\text{C}(\text{O})\text{OC}(\text{O})\text{H}$ , and  $\bullet\text{CH}_2\text{CH}_2\text{CH}_2\text{CH}_3$  radicals. Further, these  
354 radicals will react with  $\text{O}_2$  to form peroxy radicals eventually forming butyraldehyde, which was  
355 positively identified. 2) Can go through  $\alpha$ -ester rearrangement and then a C-O scission, which  
356 occurred when the H-atom abstraction is from the carbon linked to the non-carbonyl oxygen to  
357 produce a carboxylic acid and the corresponding radical coproduct. Acetic acid was identified. The  
358  $\bullet\text{C}(\text{O})(\text{CH}_2)_3\text{CH}_3$  radicals react with  $\text{O}_2$  to lead carbon dioxide and  $\bullet\text{CH}_2\text{CH}_2\text{CH}_2\text{CH}_3$  radicals. These  
359 radicals will finally form butyraldehyde.

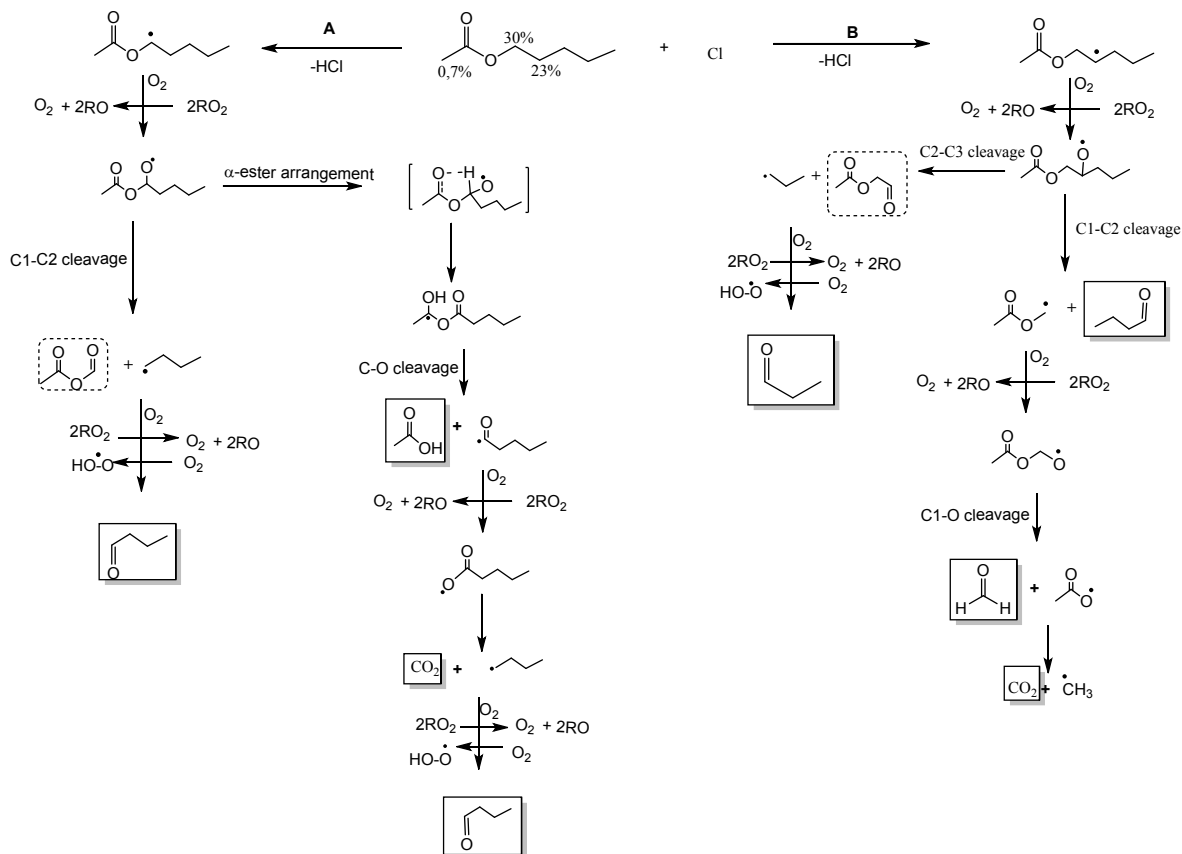
360 On the other hand, channel B shows the H-atoms abstraction from the  $-\text{CH}_2-$  ( $\text{C}_2$ ). This H abstraction  
361 generates the radical  $\text{CH}_3\text{C}(\text{O})\text{OCH}_2\text{C}(\bullet)\text{HCH}_2\text{CH}_2\text{CH}_3$  followed by  $\text{O}_2$  addition to form the peroxy  
362 radicals  $\text{CH}_3\text{C}(\text{O})\text{OCH}_2\text{C}(\text{OO}\bullet)\text{HCH}_2\text{CH}_2\text{CH}_3$  and the corresponding alkoxy radical,  
363  $\text{CH}_3\text{C}(\text{O})\text{OCH}_2\text{C}(\text{O}\bullet)\text{HCH}_2\text{CH}_2\text{CH}_3$ . These alkoxy radicals can suffer scission. If the scission occurs  
364 between  $\text{C}_1$ - $\text{C}_2$ , butyraldehyde,  $\text{CHOCH}_2\text{CH}_2\text{CH}_3$  is produced together with  $\text{CH}_3\text{C}(\text{O})\text{OC}(\bullet)\text{H}_2$   
365 radicals. These radicals react with  $\text{O}_2$  followed by  $\text{C}_1$ -O cleavage to produce formaldehyde and  $\text{CO}_2$ .  
366 In contrast, if the scission occurs between  $\text{C}_2$ - $\text{C}_3$ , 2-oxoethyl acetate,  $\text{CH}_3\text{C}(\text{O})\text{OCH}_2\text{C}(\text{O})$  is produced  
367 with  $\bullet\text{CH}_2\text{CH}_2\text{CH}_3$  radicals as coproduct. The  $\bullet\text{CH}_2\text{CH}_2\text{CH}_3$  radicals will form, propionaldehyde,  
368  $\text{CHOCH}_2\text{CH}_3$ .

369 Additionally, Scheme 2 shows two possible pathways. If the H-atoms abstraction is on the  $-\text{CH}_2-$  ( $\text{C}_3$ ),  
370 channel C, produced the radical  $\text{CH}_3\text{C}(\text{O})\text{OCH}_2\text{CH}_2\text{C}(\bullet)\text{HCH}_2\text{CH}_3$  followed by  $\text{O}_2$  addition to form  
371 the alkoxy radical  $\text{CH}_3\text{C}(\text{O})\text{OCH}_2\text{CH}_2\text{C}(\text{O}\bullet)\text{HCH}_2\text{CH}_3$ . These radicals can suffer scission. If the  
372 scission occurs between  $\text{C}_2$ - $\text{C}_3$  it is formed propionaldehyde,  $\text{CHOCH}_2\text{CH}_3$ , and  
373  $\text{CH}_3\text{C}(\text{O})\text{OCH}_2\text{C}(\bullet)\text{H}_2$  radicals. These radicals will produce formaldehyde,  $\text{CH}_2\text{O}$ , and  $\text{CO}_2$ . If the  
374 scission occurs between  $\text{C}_3$ - $\text{C}_4$  will produce the stable compound  $\text{CH}_3\text{C}(\text{O})\text{OCH}_2\text{CH}_2\text{C}(\text{O})\text{H}$ , 2-oxo-  
375 2-(3-oxopropoxy)ethan-1-ylum, and  $\bullet\text{CH}_2\text{CH}_3$  radicals. The ethyl radicals produce acetaldehyde,  
376  $\text{CHOCH}_3$ .

377 If the H-atoms abstraction is on the  $-\text{CH}_2-$  ( $\text{C}_4$ ), (channel D), will form the radical  
378  $\text{CH}_3\text{C}(\text{O})\text{OCH}_2\text{CH}_2\text{CH}_2\text{C}(\bullet)\text{HCH}_3$  followed by  $\text{O}_2$  addition to form the alkoxy radical  
379  $\text{CH}_3\text{C}(\text{O})\text{OCH}_2\text{CH}_2\text{CH}_2\text{C}(\text{O}\bullet)\text{HCH}_3$ . These radicals can undergo a cleavage between  $\text{C}_3$ - $\text{C}_4$  to lead to  
380 a stable compound, acetaldehyde,  $\text{CHOCH}_3$ , and  $\text{CH}_3\text{C}(\text{O})\text{OCH}_2\text{CH}_2\text{C}(\bullet)\text{H}_2$  radicals. These radicals  
381 could decompose to form formaldehyde and other radicals that will produce formaldehyde and  $\text{CO}_2$ .

382

383

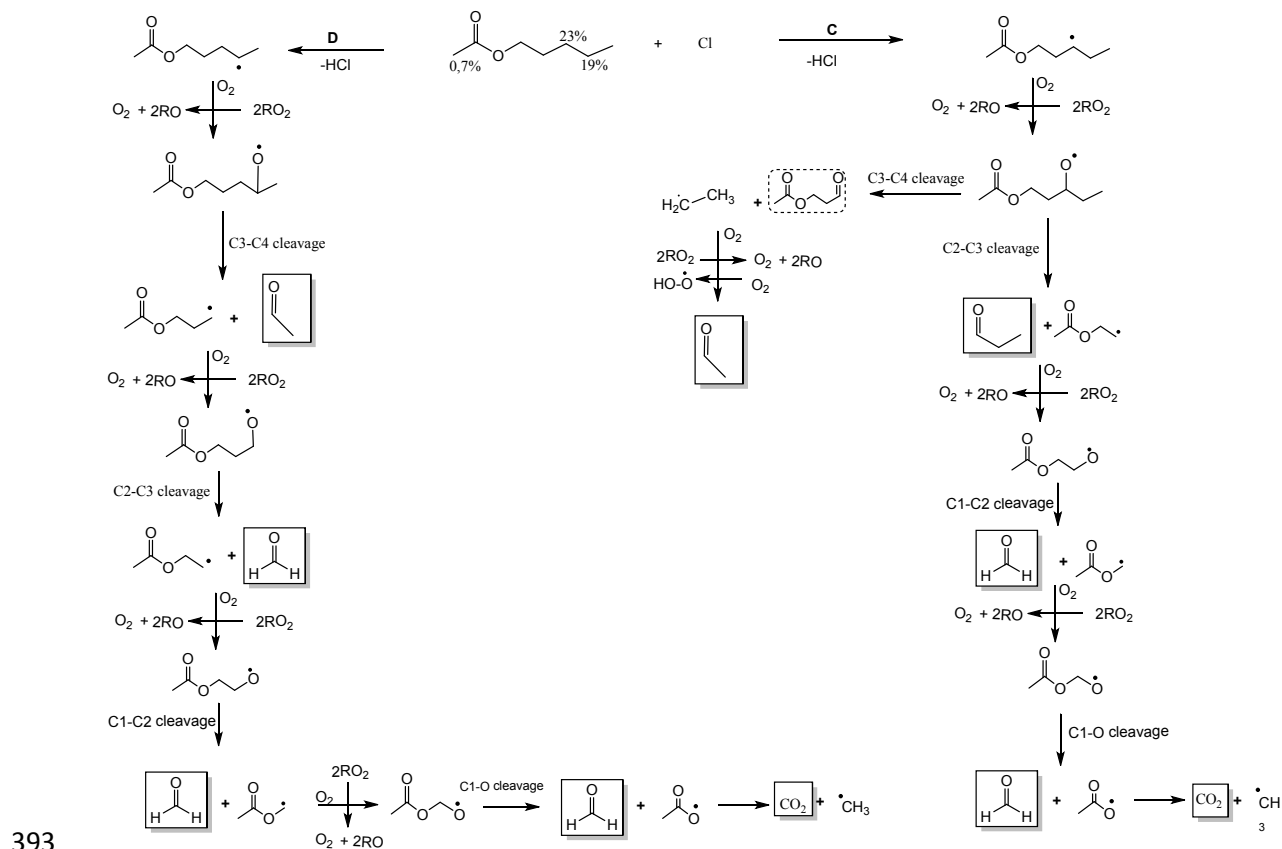


384

385 **Scheme 1.** Mechanism of Cl-atoms initiated oxidation of AA *via* H-abstraction from C<sub>1</sub> (channel A)  
 386 and C<sub>2</sub> (Channel B). Products identified in full line and unidentified products in dotted line  
 387

388 The SAR calculations predict that channel A will be the primary reaction pathway (30%), followed  
 389 by channels B and C (23%). Further studies will be necessary in order to quantify the product yields  
 390 at various conditions, such as the presence or absence of NO<sub>x</sub>, together with molecular theoretical  
 391 research, in order to fully clarify the oxidation mechanism in different atmospheric scenarios.

392



406 The rate coefficients of oxidation reactions with tropospheric oxidants such as OH radicals, Cl atoms,  
 407 O<sub>3</sub> molecules, or NO<sub>3</sub> radicals and the average tropospheric oxidant concentrations can be used to  
 408 calculate the tropospheric residence time ( $\tau$ ) by the expression  $\tau = 1/k_{AA} \times [\text{Oxidants}]$ . where [OH] is  
 409  $2.0 \times 10^6$  radicals.cm<sup>-3</sup> for about 12 hours<sup>35</sup> and [Cl] is  $(3.3 \pm 1.1) \times 10^4$  atoms.cm<sup>-3</sup> for 24 hours<sup>36</sup>

410 From Table 4, the values estimated are  $\tau_{OH} = 22$ , and  $\tau_{Cl} = 62$  hours. The short lifetime for AA in the  
 411 range of just over a few hours implies that the emission of this compound is likely to be removed  
 412 rapidly in the gas phase close to its source of emission.

413 Unfortunately, there are no kinetic data available in the literature for the reactions of this compound  
 414 with O<sub>3</sub> molecules, and NO<sub>3</sub> radicals with AA. Propyl acetate reacts with NO<sub>3</sub> with a rate coefficient  
 415 of  $(5.0 \pm 2.0) \times 10^{-17}$  cm<sup>3</sup>.molecule<sup>-1</sup>.s<sup>-1</sup> according to reported data<sup>37</sup>. It may be predicted that the rate  
 416 coefficient for AA should be on that order of magnitude with very small contribution as atmospheric  
 417 sink of this ester by reaction with NO<sub>3</sub> radicals. AA was stable to actinic radiation according to  
 418 previous photolysis investigations carried out before the kinetics experiments. These studies also did  
 419 not demonstrate a significant decrease in the signals of the FTIR.

420 **Table 4.** Atmospheric implications of AA.  
 421

Reaction	$k_{Average}$ cm <sup>3</sup> .molecule <sup>-1</sup> .s <sup>-1</sup>	$\tau$ h	[O <sub>3</sub> ] <sup>a</sup> ppm	POCP <sup>b</sup>
AA + OH	<b>(6.19 ± 1.23) × 10<sup>-12</sup></b>	22	2.15	70.2
AA + Cl	<b>(1.35 ± 0.14) × 10<sup>-10</sup></b>	62		

422 Reference compounds: <sup>a</sup>CH<sub>2</sub>=CH<sub>2</sub>=3.30 ppm; <sup>b</sup>CH<sub>2</sub>=CH<sub>2</sub>=100.

423 Due to the atmospheric lifetime, AA will probably contribute to ozone formation in local emission  
 424 areas. For this reason, the POCP, was estimated using the modeling technique described by Jenkin et  
 425 al., 2017, with equation 14, to evaluate the possible contribution of AA to the POCP.

426 
$$\text{POCP} = (A \times \gamma_S \times R \times S \times F) + P + R_{O_3} - Q \quad (14)$$

427 where, A,  $\gamma_s$ , R, and S are core parameters used for all VOCs, F, P, R<sub>O3</sub> and Q are parameters used for  
 428 specific groups of compounds, and which otherwise take default values of 1 for F or 0 for P, R<sub>O3</sub>, and  
 429 Q. The parameter A is a multiplier and  $\gamma_s$  is a variable connected to the VOC's structure.

430 With this method, the POCPs<sup>38</sup> of VOCs are calculated in relation to ethane, which is given a value  
 431 of 100. The estimated POCP value for AA is 70.2. It can be observed that, in comparison to ethane  
 432 as a reference compound, AA has significant risk of contributing to photochemical smog.  
 433 Furthermore, using the reported<sup>39</sup> Dash et al., 2013 equation (15), it was estimated the [O<sub>3</sub>] during the  
 434 reaction of VOCs with OH radicals.

$$435 \quad O_3 = \frac{n'[k_a(OH)]^2}{4.6[2.7 \times 10^{-5} - k(OH)]} \times \left( \frac{1}{k_a(OH)} - \frac{1 - e^{-1.24 \times 10^{-4}/k_a(OH)}}{2.7 \times 10^{-5}} \right) \quad (15)$$

436 where n' is the maximum possible ozone molecules that can be produced from one molecule of VOC  
 437 based on the number of nC + nH atoms present in that molecule,  $k_a$  is the rate coefficient, and (OH)  
 438 is the global weighted-average OH radical concentration. The average ozone production during the  
 439 reaction of AA with OH radicals was estimated to be 2.15 ppm. This value can be compared with of  
 440 ethene value, 3.30 ppm. Due to the close values, the degradation of AA could have a negative impact  
 441 on human health since it will increase the tropospheric ozone.

442 The release of AA into the atmosphere can contribute to the overall chemical composition of the air.  
 443 In small quantities, it is unlikely to have a significant impact on air quality. However, if large amounts  
 444 of AA are released, either from industrial processes, it can contribute to the formation of secondary  
 445 pollutants such as ozone or particulate matter. AA can degrade in the atmosphere to produce a number  
 446 of VOCs with different impacts on the troposphere and the surface of the Planet.

447 Small aldehydes, such as formaldehyde ( $\text{CH}_2\text{O}$ ) and acetaldehyde ( $\text{CH}_3\text{CHO}$ ), can have atmospheric  
448 implications due to their reactivity. These aldehydes are highly reactive compounds in the atmosphere.  
449 They can participate in photochemical reactions, reacting with other atmospheric constituents such  
450 as hydroxyl radicals ( $\text{OH}$ ) and nitrogen oxides ( $\text{NO}_x$ )<sup>40,41</sup>. These reactions can contribute to the  
451 formation of secondary pollutants, including peroxyacyl nitrates (PANs) and ozone ( $\text{O}_3$ ), which can  
452 impact air quality. Both formaldehyde and acetaldehyde are known to contribute to the formation of  
453 ground-level ozone, which are a harmful pollutant and a component of smog. They can also contribute  
454 to the formation of secondary organic aerosols, which have implications for air quality and human  
455 health. Formaldehyde is classified as a human carcinogen by the International Agency for Research  
456 on Cancer (IARC)<sup>42</sup>, and it can cause respiratory irritation and other health issues. Acetaldehyde is a  
457 respiratory irritant and is also classified as a potential carcinogen. For this reason, numerous field  
458 studies are carried out to evaluate the levels of carbonyl VOCs as main pollutants in the atmosphere  
459 of populated cities and their potential risk to health<sup>43,44</sup>.

460 Acetic acid is readily soluble in water, and its fate in the atmosphere depends on various factors such  
461 as temperature, humidity, and reaction rates. It can undergo oxidation reactions to form other organic  
462 compounds or be scavenged by precipitation and deposited onto the Earth's surface.

463

464

## 465 **5 Conclusions**

466 Once released into the atmosphere, AA can undergo various chemical reactions. It can be degraded  
467 by reactions with hydroxyl radicals or other oxidizing agents present in the atmosphere. The exact  
468 fate of AA will depend on the specific conditions of the environment, such as the presence of sunlight,  
469 other pollutants, and the atmospheric concentrations of reactive species.

470 The residence time of AA is around 22 hours for reaction with OH radicals and 62 hours in reaction  
471 with Cl atoms. It would have a regional and local impact.

472 The degradation mechanism initiated by the Cl atoms is similar that OH radicals by H-atoms  
473 abstraction from the alkyl groups followed by O<sub>2</sub> addition to form the peroxy radicals further alkoxy  
474 radical's formation. The fate of alkoxy radicals depends on several reaction pathways.

475 AA can degrade in the atmosphere to produce a number of VOCs as acetic acid, formaldehyde,  
476 acetaldehyde, propionaldehyde, and butyraldehyde with different impacts on the troposphere. Small  
477 aldehydes can contribute to produces other pollutants, such as peroxyacyl nitrates (PANs) and ozone  
478 (O<sub>3</sub>).

479 The reaction of OH radicals with AA might have a harmful effect on human health since it will cause  
480 the creation of a considerable amount of tropospheric ozone and has a significant risk of contributing  
481 to photochemical smog.

## 482 **Conflicts of interest**

483 There are no conflicts to declare.

## 484 **Acknowledgements**

485 The authors wish to acknowledge to EUROCHAMP 2020, FONCyT, CONICET and SECyT UNC,  
486 Argentina. M. B. B. wish to acknowledge the Alexander von Humboldt Foundation for financial  
487 support. V.G.S.C wishes to acknowledge to CONICET for a doctoral fellowship and support.

## 488 **References**

- 489 1 R. Atkinson, Gas-phase tropospheric chemistry of organic compounds: a review, *Atmospheric Environment*,  
490 2007, **41**, 200–240.
- 491 2 A. El Boudali, S. Le Calvé, G. Le Bras and A. Mellouki, Kinetic Studies of OH Reactions with a Series of  
492 Acetates, *J. Phys. Chem.*, 1996, **100**, 12364–12368.
- 493 3 1: Final Report on the Safety Assessment of Amyl Acetate and Isoamyl Acetate, *Journal of the American*  
494 *College of Toxicology*, 1988, **7**, 705–719.
- 495 4 I. Barnes, K. H. Becker and N. Mihalopoulos, An FTIR product study of the photooxidation of dimethyl  
496 disulfide, *J Atmos Chem*, 1994, **18**, 267–289.
- 497 5 R. Atkinson, D. L. Baulch, R. A. Cox, R. F. Hampson, J. A. Kerr, M. J. Rossi and J. Troe, Evaluated Kinetic,  
498 Photochemical and Heterogeneous Data for Atmospheric Chemistry: Supplement V. IUPAC Subcommittee



- 499 on Gas Kinetic Data Evaluation for Atmospheric Chemistry, *Journal of Physical and Chemical Reference*  
500 *Data*, 1997, **26**, 521–1011.
- 501 6 A. Bonard, V. Daële, J.-L. Delfau and C. Vovelle, Kinetics of OH Radical Reactions with Methane in the  
502 Temperature Range 295–660 K and with Dimethyl Ether and Methyl-tert-butyl Ether in the Temperature  
503 Range 295–618 K, *J. Phys. Chem. A*, 2002, **106**, 4384–4389.
- 504 7 Evaluated kinetic and photochemical data for atmospheric chemistry: Supplement IV: IUPAC subcommittee  
505 on gas kinetic data evaluation for atmospheric chemistry - ScienceDirect,  
506 <https://www.sciencedirect.com/science/article/abs/pii/096016869290383V>, (accessed 17 March 2023).
- 507 8 E. C. Tuazon, R. Atkinson, S. M. Aschmann, M. A. Goodman and A. M. Winer, Atmospheric reactions of  
508 chloroethenes with the OH radical, *Int. J. Chem. Kinet.*, 1988, **20**, 241–265.
- 509 9 R. Atkinson and S. M. Aschmann, Kinetics of the gas-phase reactions of Cl atoms with chloroethenes at  
510  $298 \pm 2$  K and atmospheric pressure, *Int. j. chem. kinet.*, 1987, **19**, 1097–1105.
- 511 10 O. US EPA, EPI Suite™-Estimation Program Interface, [https://www.epa.gov/tsca-screening-tools/epi-](https://www.epa.gov/tsca-screening-tools/epi-suite-estimation-program-interface)  
512 [suite-estimation-program-interface](https://www.epa.gov/tsca-screening-tools/epi-suite-estimation-program-interface), (accessed 23 March 2023).
- 513 11 D. C. Williams, L. N. O'Rji and D. A. Stone, Kinetics of the reactions of OH radicals with selected acetates  
514 and other esters under simulated atmospheric conditions, *Int. J. Chem. Kinet.*, 1993, **25**, 539–548.
- 515 12 Antonia Zogka. Atmospheric degradation of a series of methoxy and ethoxy acetates and n-pentyl acetate.  
516 Other. Université d'Orléans, 2016. English. NNT : 2016ORLE2071. tel-01581321.
- 517 13 S. Ifang, T. Benter and I. Barnes, Reactions of Cl atoms with alkyl esters: kinetic, mechanism and  
518 atmospheric implications, *Environ Sci Pollut Res*, 2015, **22**, 4820–4832.
- 519 14 L. N. Farrugia, I. Bejan, S. C. Smith, D. J. Medeiros and P. W. Seakins, Revised structure activity parameters  
520 derived from new rate coefficient determinations for the reactions of chlorine atoms with a series of seven  
521 ketones at 290K and 1atm, *Chemical Physics Letters*, 2015, **640**, 87–93.
- 522 15 S. M. Aschmann and R. Atkinson, Rate constants for the gas-phase reactions of alkanes with Cl atoms at  
523  $296 \pm 2$  K: GAS-PHASE REACTIONS OF ALKANES, *Int. J. Chem. Kinet.*, 1995, **27**, 613–622.
- 524 16 J.-H. Xing, K. Takahashi, M. D. Hurley and T. J. Wallington, Kinetics of the reactions of chlorine atoms  
525 with a series of acetates, *Chemical Physics Letters*, 2009, **474**, 268–272.
- 526 17 R. Atkinson, Kinetics and mechanisms of the gas-phase reactions of the hydroxyl radical with organic  
527 compounds under atmospheric conditions, *Chem. Rev.*, 1986, **86**, 69–201.
- 528 18 G. S. Tyndall, A. S. Pimentel and J. J. Orlando, Temperature Dependence of the Alpha-Ester Rearrangement  
529 Reaction, *J. Phys. Chem. A*, 2004, **108**, 6850–6856.
- 530 19 B. Picquet, S. Heroux, A. Chebbi, J.-F. Doussin, R. Durand-Jolibois, A. Monod, H. Loirat and P. Carlier,  
531 Kinetics of the reactions of OH radicals with some oxygenated volatile organic compounds under simulated  
532 atmospheric conditions, *Int. J. Chem. Kinet.*, 1998, **30**, 839–847.
- 533 20 C. Ferrari, A. Roche, V. Jacob, P. Foster and P. Baussand, Kinetics of the reaction of OH radicals with a  
534 series of esters under simulated conditions at 295 K, *Int. J. Chem. Kinet.*, 1996, **28**, 609–614.
- 535 21 M. Veillerot, P. Foster, R. Guillermo and J. C. Galloo, Gas-phase reaction of n-butyl acetate with the  
536 hydroxyl radical under simulated tropospheric conditions: Relative rate constant and product study, *Int. J.*  
537 *Chem. Kinet.*, 1996, **28**, 235–243.
- 538 22 L. K. Christensen, J. C. Ball and T. J. Wallington, Atmospheric Oxidation Mechanism of Methyl Acetate,  
539 *J. Phys. Chem. A*, 2000, **104**, 345–351.
- 540 23 M. T. Baumgartner, R. A. Taccone, M. A. Teruel and S. I. Lane, Theoretical study of the relative reactivity  
541 of chloroethenes with atmospheric oxidants (OH, NO<sub>3</sub>, O(3P), Cl(2P) and Br(2P)), *Phys. Chem. Chem.*  
542 *Phys.*, 2002, **4**, 1028–1032.
- 543 24 M. B. Blanco, I. Bejan, I. Barnes, P. Wiesen and M. A. Teruel, Temperature-dependent rate coefficients for  
544 the reactions of Cl atoms with methyl methacrylate, methyl acrylate and butyl methacrylate at atmospheric  
545 pressure, *Atmospheric Environment*, 2009, **43**, 5996–6002.
- 546 25 N. Schütze, X. Zhong, S. Kirschbaum, I. Bejan, I. Barnes and T. Benter, Relative kinetic measurements of  
547 rate coefficients for the gas-phase reactions of Cl atoms and OH radicals with a series of methyl alkyl esters,  
548 *Atmospheric Environment*, 2010, **44**, 5407–5414.
- 549 26 S. Le Calvé, G. Le Bras and A. Mellouki, Kinetic Studies of OH Reactions with a Series of Methyl Esters,  
550 *J. Phys. Chem. A*, 1997, **101**, 9137–9141.
- 551 27 V. F. Andersen, K. B. Ørnsø, S. Jørgensen, O. J. Nielsen and M. S. Johnson, Atmospheric Chemistry of  
552 Ethyl Propionate, *J. Phys. Chem. A*, 2012, **116**, 5164–5179.

- 553 28 P. M. Cometto, V. Daële, M. Idir, S. I. Lane and A. Mellouki, Reaction Rate Coefficients of OH Radicals  
554 and Cl Atoms with Ethyl Propanoate, *n* -Propyl Propanoate, Methyl 2-Methylpropanoate, and Ethyl *n* -  
555 Butanoate, *J. Phys. Chem. A*, 2009, **113**, 10745–10752.
- 556 29 F. Taketani, Y. Matsumi, T. J. Wallington and M. D. Hurley, Kinetics of the gas phase reactions of chlorine  
557 atoms with a series of ketones, *Chemical Physics Letters*, 2006, **431**, 257–260.
- 558 30 R. Atkinson, S. M. Aschmann, W. P. L. Carter and J. N. Pitts, Rate constants for the gas-phase reaction of  
559 OH radicals with a series of ketones at  $299 \pm 2$  K: REACTION OF OH RADICALS AND KETONES, *Int.*  
560 *J. Chem. Kinet.*, 1982, **14**, 839–847.
- 561 31 E. Jiménez, B. Ballesteros, E. Martínez and J. Albaladejo, Tropospheric Reaction of OH with Selected  
562 Linear Ketones: Kinetic Studies between 228 and 405 K, *Environ. Sci. Technol.*, 2005, **39**, 814–820.
- 563 32 S. Lin and J. March, March's Advanced Organic Chemistry: Reactions, Mechanisms, and Structure, 5th  
564 Edition, *Molecules*, 2001, **6**, 1064–1065.
- 565 33 N. O. of D. and Informatics, Libro del Web de Química del NIST, <https://webbook.nist.gov/chemistry/>,  
566 (accessed 14 July 2023).
- 567 34 M. B. Blanco and M. A. Teruel, Atmospheric degradation of fluoroesters (FESs): Gas-phase reactivity study  
568 towards OH radicals at 298K, *Atmospheric Environment*, 2007, **41**, 7330–7338.
- 569 35 R. Hein, P. J. Crutzen and M. Heimann, An inverse modeling approach to investigate the global atmospheric  
570 methane cycle, *Global Biogeochemical Cycles*, 1997, **11**, 43–76.
- 571 36 O. W. Wingenter, M. K. Kubo, N. J. Blake, T. W. Smith Jr., D. R. Blake and F. S. Rowland, Hydrocarbon  
572 and halocarbon measurements as photochemical and dynamical indicators of atmospheric hydroxyl, atomic  
573 chlorine, and vertical mixing obtained during Lagrangian flights, *Journal of Geophysical Research:*  
574 *Atmospheres*, 1996, **101**, 4331–4340.
- 575 37 S. Langer, E. Ljungström and I. Wängberg, Rates of reaction between the nitrate radical and some aliphatic  
576 esters, *J. Chem. Soc., Faraday Trans.*, 1993, **89**, 425–431.
- 577 38 M. E. Jenkin, R. G. Derwent and T. J. Wallington, Photochemical ozone creation potentials for volatile  
578 organic compounds: Rationalization and estimation, *Atmospheric Environment*, 2017, **163**, 128–137.
- 579 39 M. R. Dash and B. Rajakumar, Experimental and theoretical rate coefficients for the gas phase reaction of  
580  $\beta$ -Pinene with OH radical, *Atmospheric Environment*, 2013, **79**, 161–171.
- 581 40 R. Atkinson, D. L. Baulch, R. A. Cox, J. N. Crowley, R. F. Hampson, R. G. Hynes, M. E. Jenkin, M. J.  
582 Rossi and J. Troe, Evaluated kinetic and photochemical data for atmospheric chemistry: Volume III ? gas  
583 phase reactions of inorganic halogens, *Atmospheric Chemistry and Physics*, 2007, **7**, 981–1191.
- 584 41 R. Atkinson, C. N. Plum, W. P. L. Carter, A. M. Winer and J. N. Pitts, Rate constants for the gas-phase  
585 reactions of nitrate radicals with a series of organics in air at  $298 \pm 1$  K, *J. Phys. Chem.*, 1984, **88**, 1210–  
586 1215.
- 587 42 IARC, *Formaldehyde, 2-Butoxyethanol and 1-tert-Butoxypropan-2-ol*. IARC Monographs on the  
588 *Evaluation of Carcinogenic Risks to Humans Volume 88*, Lyon, France, 2006, vol. 88.
- 589 43 F. Villanueva, A. Tapia, A. Notario, J. Albaladejo and E. Martínez, Ambient levels and temporal trends of  
590 VOCs, including carbonyl compounds, and ozone at Cabañeros National Park border, Spain, *Atmospheric*  
591 *Environment*, 2014, **85**, 256–265.
- 592 44 Y.-Y. Lu, Y. Lin, H. Zhang, D. Ding, X. Sun, Q. Huang, L. Lin, Y.-J. Chen, Y.-L. Chi and S. Dong,  
593 Evaluation of Volatile Organic Compounds and Carbonyl Compounds Present in the Cabins of Newly  
594 Produced, Medium- and Large-Size Coaches in China, *Int J Environ Res Public Health*, 2016, **13**, 596.
- 595